Quantum Electronics **37** (3) 209 – 230 (2007)

INVITED PAPER

PACS numbers: 32.50.+d; 78.67.Bf; 36.40.Jn
DOI: 10.1070/QE2007v037n03ABEH013322

Optical properties of an atom in the presence of a two-nanosphere cluster

V.V. Klimov, D.V. Guzatov

Contents

Abstract. **The optical properties of an atom located near a cluster of two arbitrarily arranged nanospheres of an arbitrary composition are studied. Changes in the spontaneous decay rates of excited states and emission frequency shifts are considered for different orientations of the dipole moment and different positions of the atom with respect to the cluster. It is shown that a two-nanosphere cluster can be used to control efficiently the spontaneous decay rates of excited states of the atom by changing the distance between spheres. It is found that spontaneous decay rates of the excited states of an atom located between silver nanospheres and having the dipole moment directed along the axis connecting the centres of spheres can increase by a factor of 10^5 and more when nanospheres are brought closer together.**

Keywords: *nanooptics, nanoplasmonics, spectroscopy, nanoparticles.*

V.V. Klimov, D.V. Guzatov P.N. Lebedev Physics Institute, Russian Academy of Sciences, Leninsky prosp. 53, 119991 Moscow, Russia; e-mail: vklim@sci.lebedev.ru

Received 19 June 2006
Kvantovaya Elektronika **37** (3) 209 – 230 (2007)
Translated by M.N. Sapozhnikov

1. Introduction

Recently a great number of papers devoted to investigations of the spectroscopic parameters of a dipole source (atom, molecule) in the presence of meso- and nanostructures appeared. From the theoretical point of view, this problem is quite challenging because an atom interacts with optical fields that are strongly inhomogeneous at the nanometre scale. In the case of plasmon – polariton [1, 2] and phonon – polariton [3] resonances, the local field increases very strongly. Some possible applications based on this effect were considered. Applications in which strong local fields near irregular surfaces are used to increase Raman scattering cross section are most developed at present [4]. Changes in the properties of emitting atoms located near nanobodies of different shapes and different compositions are used in nanobiosensors [5 – 7], nanolasers [8], microscopes for the observation of individual molecules [9], devices for decoding the DNA structure [10], chemical sensors [11 – 13], and many other devices [14]. At present the optical properties of atoms located near individual nanospheres, nanowires, and nanospheroids are studied in detail [15 – 18]. Note also paper [19] devoted to the study of the radiative decay rate of the excited state of an atom located near a three-axial ellipsoid, which can be used for the development of new types of artificial fluorophores.

Investigations of the optical properties of clusters

consisting of two and more metal nanoparticles are especially promising because a change in the cluster geometry allows the efficient control of the plasmon (phonon) spectrum. The optical properties of clusters consisting of two nanoparticles were studied in a number of theoretical [20–32] and experimental [33–36] papers. The case of nearly touching nanoparticles is the most interesting because the local field especially strongly increases in the gap between the nanoparticles, and at the same time this case is the most complicated. The interaction of an atom with a cluster of nanoparticles results in the excitation of special plasmon oscillations [21], which are strongly localised between spheres and vanish at large distances.

The aim of this paper is to study the optical properties of an atom (or a molecule) near a cluster of two arbitrarily arranged spherical nanoparticles of an arbitrary size (Fig. 1). In section 2, we discuss briefly the specific features of the theory of spontaneous emission of an atom located near nanobodies. In section 3, the solution of the quasistatic problem is obtained for an electric field produced by the atom near the cluster. The analytic solution is presented for the case of ideally conducting nanospheres. In section 4, the resonance properties of a cluster of two metal nanospheres, or more exactly, two spheres made of a material with the dielectric constant $\varepsilon < 0$ are considered. Section 5 is devoted to the study of the spontaneous decay rate of the excited state of an atom located near a cluster. General equations are obtained for arbitrarily arranged spheres of an arbitrary composition. Asymptotic expressions for the spontaneous decay rate are studied at large and small distances between nanospheres. At the end of section 5, graphic results are presented and discussed. In section 6, the frequency shift of the atomic emission in the presence of a cluster is studied, asymptotic expressions for the frequency shift are considered at small and large distances between spheres, and the results are graphically illustrated and discussed.

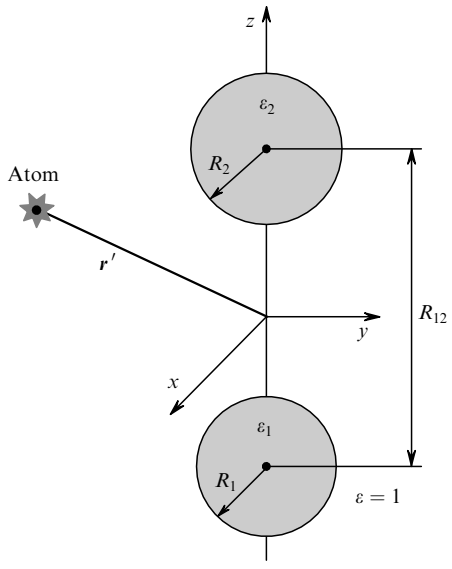

Figure 1. Geometry of the problem.

2. Elements of the theory of spontaneous emission of an atom in the presence of nanobodies

In the case of a weak interaction between an atom and a nanobody, i.e. when the spontaneous decay is exponential, the width γ_a of the excited level a of the atom located at point $\boldsymbol{r} = \boldsymbol{r}'$ (hereafter, primed coordinates denote the position of an atom) is described by the expression [37]

$$\gamma_a = \gamma_{0a} + \frac{2}{\hbar}\sum_n d_{0\alpha}^{(an)} d_{0\beta}^{(na)} \operatorname{Im} G_{\alpha\beta}(\boldsymbol{r}', \boldsymbol{r}'; \omega_{na})\Theta(\omega_{an}), \quad (1)$$

where γ_{0a} is the level width in a free space in the absence of a nanobody; $d_{0\alpha}^{(an)}$ is the matrix element of the dipole momentum operator between the states a and n; $\omega_{na} = (W_n - W_a)/\hbar$ is the frequency of transition between the states n and a; $G_{\alpha\beta}$ is the reflected part of the Green function of the classical problem, which is related to the reflected field E_α^{r} by the expression

$$E_\alpha^{\mathrm{r}}(\boldsymbol{r}) = G_{\alpha\beta}(\boldsymbol{r}, \boldsymbol{r}'; \omega_{na}) d_{0\beta}^{(na)}; \quad (2)$$

$\alpha, \beta = x, y, z$ (hereafter, summation is assumed over repeated indices); and Θ is the Heaviside function. We will study below the emission linewidth by considering only one of the excited-state decay channels, for example, the $e \to g$ transition. To take into account the possible decay to different states, it is only necessary to sum the partial linewidths of all possible transitions. The expression for the relative linewidth, i.e. the linewidth normalised to the linewidth in a free space obtained in the classical (Lorentz) theory of an atom [38, 39] coincides with corresponding quantum-mechanical expression (1).

The expression for the energy level shift δW_a for an arbitrary state a of an atom has the form [40]

$$\delta W_a = \delta W_a^{\mathrm{cl}} + \delta W_a^{\mathrm{vdW}}, \quad (3)$$

where

$$\delta W_a^{\mathrm{cl}} = -\sum_n d_{0\alpha}^{(an)} d_{0\beta}^{(na)} \operatorname{Re} G_{\alpha\beta}(\boldsymbol{r}', \boldsymbol{r}'; \omega_{na})\Theta(\omega_{an});$$
$$\delta W_a^{\mathrm{vdW}} = -\frac{\hbar}{2\pi}\int_0^\infty \mathrm{d}\xi G_{\alpha\beta}(\boldsymbol{r}', \boldsymbol{r}'; \omega = \mathrm{i}\xi)\Pi_{\alpha\beta}^{(a)}(\omega = \mathrm{i}\xi); \quad (4)$$

and

$$\Pi_{\alpha\beta}^{(a)}(\omega) = \frac{2}{\hbar}\sum_n \frac{\omega_{na} d_{0\alpha}^{(an)} d_{0\beta}^{(na)}}{\omega_{na}^2 - (\omega + \mathrm{i}0^+)^2} \quad (5)$$

is the polarisability of the state a. Note that expressions (1) and (3) were obtained by using the most general assumptions and therefore the field of their applications is very broad.

Thus, the problem of determining the spectral parameters of an atom near any body is reduced to the calculation of the reflected field or the Green function and analysis of expressions (1) and (4).

In the case of nanobodies, the perturbation theory over a small parameter $2\pi b/\lambda \ll 1$ can be often used, where b is the characteristic size of a nanobody and λ is the emission wavelength (Rayleigh theory). In this case, the Green

function of the reflected field can be expanded as a power series in the wave number k:

$$G_{\alpha\beta}(\boldsymbol{r},\boldsymbol{r}';\omega) = G^{(0)}_{\alpha\beta}(\boldsymbol{r},\boldsymbol{r}') + kG^{(1)}_{\alpha\beta}(\boldsymbol{r},\boldsymbol{r}') + k^2G^{(2)}_{\alpha\beta}(\boldsymbol{r},\boldsymbol{r}') + \mathrm{i}k^3G^{(3)}_{\alpha\beta}(\boldsymbol{r},\boldsymbol{r}') + \ldots, \tag{6}$$

where $G^{(j)}_{\alpha\beta}$ $(j = 0, 1, 2, \ldots)$ are coefficients, which can be found by solving the corresponding quasi-static problems [41], and $k = \omega/c$. Note that the dependence $\varepsilon(\omega)$ should not be taken into account in expansion (6). The first three terms in (6) describe near fields, while the higher-order terms describe emission fields. By substituting expansion (6) into (1), we obtain the total rate of spontaneous transition from the state e to the state g near a nanobody

$$\gamma = \underbrace{\frac{2}{\hbar}\, d^{(eg)}_{0\alpha} d^{(ge)}_{0\beta} \mathrm{Im}\left[G^{(0)}_{\alpha\beta}(\boldsymbol{r}',\boldsymbol{r}') + \ldots\right]}_{\text{nonradiative losses}} + \underbrace{\gamma_0 + \frac{2}{\hbar}\, d^{(eg)}_{0\alpha} d^{(ge)}_{0\beta} \mathrm{Re}\left[k_0^3 G^{(3)}_{\alpha\beta}(\boldsymbol{r}',\boldsymbol{r}') + \ldots\right]}_{\text{radiative losses}}, \tag{7}$$

where $k_0 = \omega_{eg}/c$; γ_0 is the transition linewidth in the absence of a nanobody. The first term in (7) is nonzero only for absorbing media and describes nonradiative losses, while the rest of the terms are nonzero in the absence of absorption as well. These terms describe mainly radiative losses. Therefore, to find the leading terms of nonradiative and radiative losses, it is necessary to calculate $G^{(0)}_{\alpha\beta}(\boldsymbol{r}',\boldsymbol{r}')$ and $G^{(3)}_{\alpha\beta}(\boldsymbol{r}',\boldsymbol{r}')$, respectively.

To find the term describing nonradiative losses, it is sufficient to solve the quasi-static electrodynamic problem with a dipole source. The direct determination of radiative losses described by the third-order terms in k is a complicated problem. However, if an atom is located close to a nanobody, emission has the dipole nature, and the total dipole moment of the atom + nanobody system can be again found from the analysis of the function $G^{(0)}_{\alpha\beta}(\boldsymbol{r},\boldsymbol{r}')$ at large distances from the system. Thus, the radiative width of the $e \to g$ transition line in the presence of nanobodies is described by the expression

$$\left(\frac{\gamma}{\gamma_0}\right)^{\mathrm{rad}} = \frac{|\boldsymbol{d}_{\mathrm{tot}}|^2}{d_0^2}, \tag{8}$$

where $\boldsymbol{d}_{\mathrm{tot}} = \boldsymbol{d}_0 + \delta\boldsymbol{d}$ is the total dipole moment of the atom + nanobody system; $\boldsymbol{d}_0$ is the vector of the transition dipole moment; and $\delta\boldsymbol{d}$ is the induced dipole moment. It can be shown that expression (8) is valid within the framework of the quantum-mechanical approach [17].

Similarly, by substituting expansion (6) into expression (3) for the level shift in any state a, we can obtain the relation

$$\delta W_a = -\frac{1}{2}\langle a|d_{0\alpha}d_{0\beta}|a\rangle \mathrm{Re}\left[G^{(0)}_{\alpha\beta}(\boldsymbol{r}',\boldsymbol{r}')\right] - \frac{1}{2}\sum_n d^{(an)}_{0\alpha} d^{(na)}_{0\beta} \mathrm{Im}\left[G^{(0)}_{\alpha\beta}(\boldsymbol{r},\boldsymbol{r}')\right] \frac{\omega_{an}}{|\omega_{an}|} + \ldots. \tag{9}$$

In the case of a substance with low losses, the second term in (9) can be always neglected compared to the first one. Then, the frequency shift of the $e \to g$ transition in an atom located near a nanobody has the form

$$\Delta\omega = -\frac{1}{2\hbar}\left(\langle e|d_{0\alpha}d_{0\beta}|e\rangle - \langle g|d_{0\alpha}d_{0\beta}|g\rangle\right)\mathrm{Re}\left[G^{(0)}_{\alpha\beta}(\boldsymbol{r}',\boldsymbol{r}')\right] + \ldots. \tag{10}$$

As a result, to find a change in the spontaneous decay rate and frequency shifts in the presence of any nanoobject with low losses ($\varepsilon'' \ll \varepsilon'$, $\varepsilon = \varepsilon' + \mathrm{i}\varepsilon''$) whose dimensions are small compared to the emission wavelength, it is sufficient to solve the quasi-static problem for a dipole located near this nanoobject and find the function $G^{(0)}_{\alpha\beta}(\boldsymbol{r},\boldsymbol{r}')$. According to (10) and (7), the value of this function for coinciding arguments will give the frequency shift and nonradiative component of the transition rate, respectively, while the dipole moment, found from the asymptotic of this function at infinity, will give, according to (8), the radiative decay rate.

3. Quasi-static problem for a dipole near a two-nanosphere cluster

To find the leading terms of asymptotic expressions for the spontaneous decay rate and the frequency shift of emission of an atom in the presence of an arbitrary nanobody, it is sufficient to solve the quasi-static problem for the potential Φ of an atom located near a nanobody:

$$\boldsymbol{E} = -\nabla\Phi, \qquad \Delta\Phi = 4\pi\exp(-\mathrm{i}\omega t)(\boldsymbol{d}_0\nabla')\delta(\boldsymbol{r}-\boldsymbol{r}'), \tag{11}$$

where ∇, ∇' are gradients along the coordinates $\boldsymbol{r}$ and $\boldsymbol{r}'$, respectively, and Δ is the Laplace operator. We will further omit the exponential factor $\exp(-\mathrm{i}\omega t)$.

It is convenient to solve Eqn (11) in the case of two nanospheres in the bispherical coordinate system (Fig. 2). The coordinates of the bispherical system $-\infty < \eta < \infty$, $0 < \xi \leqslant \pi$, and $0 \leqslant \varphi < 2\pi$ are related to the Cartesian coordinates by expressions [42, 43]

$$x = f\frac{\sin\xi\cos\varphi}{\cosh\eta - \cos\xi}, \quad y = f\frac{\sin\xi\sin\varphi}{\cosh\eta - \cos\xi}, \quad z = f\frac{\sinh\eta}{\cosh\eta - \cos\xi}. \tag{12}$$

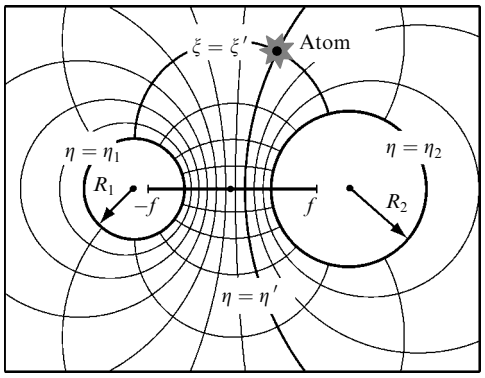

Figure 2. Bispherical coordinates.

The relation $\eta = \eta_1 < 0$ specifies a sphere of radius $R_1 = f/|\sinh\eta_1|$ in the Cartesian coordinate system. Its centre is located at the point with coordinates $x_1 = y_1 = 0$, $z_1 = f\times\coth\eta_1$. The second sphere can be specified similarly by the expression $\eta = \eta_2 > 0$. The radius of this sphere is $R_2 = f/\sinh\eta_2$ and its centre is located at the point with coordinates $x_2 = y_2 = 0$, $z_2 = f\coth\eta_2$. The dimensional constant f is half the distance between the poles of the bispherical coordinate system. It is defined by the positive root of the equation $R_{12} = (R_1^2 + f^2)^{1/2} + (R_2^2 + f^2)^{1/2}$, where $R_{12} = z_2 - z_1$ is the distance between the centres of the first and second spheres, which, as the radii of spheres, is defined arbitrarily ($R_{12} \geqslant R_1 + R_2$).

Equation (11) for the potential $\Phi = (\boldsymbol{d}_0\nabla')\tilde{\Phi}$ can be written in the more convenient form

$$\Delta\tilde{\Phi} = 4\pi\delta(\boldsymbol{r} - \boldsymbol{r}'). \tag{13}$$

The solution of Eqn (13) has the form

$$\tilde{\Phi} = \tilde{\Phi}^{\mathrm{r}} + G_0, \tag{14}$$

where $\tilde{\Phi}^{\mathrm{r}}$ is the potential of the reflected field produced by the point unit charge, and G_0 is the Green function of the point unit charge in a free space. The expression for G_0 in the bispherical coordinate system can be represented in the form [42, 43]

$$G_0(\boldsymbol{r},\boldsymbol{r}') = \frac{1}{|\boldsymbol{r}-\boldsymbol{r}'|} = \frac{1}{f}(\cosh\eta - \cos\xi)^{1/2} \times \sum_{n=0}^{\infty}\sum_{m=0}^{n}\exp\left[-\left(n+\frac{1}{2}\right)|\eta-\eta'|\right]P_n^m(\cos\xi) \times (c_{mn}\cos m\varphi + d_{mn}\sin m\varphi), \tag{15}$$

where

$$\begin{pmatrix} c_{mn} \\ d_{mn} \end{pmatrix} = [2-\delta(m,0)]\frac{(n-m)!}{(n+m)!}(\cosh\eta' - \cos\xi')^{1/2} \times P_n^m(\cos\xi')\begin{pmatrix} \cos m\varphi' \\ \sin m\varphi' \end{pmatrix}; \tag{16}$$

P_n^m are the associated Legendre functions and $\delta(m,0)$ is the Kronecker delta.

We will seek the induced potential $\tilde{\Phi}^{\mathrm{r}}$ outside spheres ($\eta_1 < \eta < \eta_2$) in the form

$$\tilde{\Phi}^{\mathrm{r}} = \frac{1}{f}(\cosh\eta - \cos\xi)^{1/2}\sum_{n=0}^{\infty}\sum_{m=0}^{n}P_n^m(\cos\xi) \times \left\{\left\{\alpha_{mn}\cosh\left[\left(n+\frac{1}{2}\right)\eta\right] + \gamma_{mn}\sinh\left[\left(n+\frac{1}{2}\right)\eta\right]\right\}\cos m\varphi + \left\{\beta_{mn}\cosh\left[\left(n+\frac{1}{2}\right)\eta\right] + \delta_{mn}\sinh\left[\left(n+\frac{1}{2}\right)\eta\right]\right\}\sin m\varphi\right\}. \tag{17}$$

Potentials inside the first ($\eta < \eta_1 < 0$) and second ($\eta > \eta_2 > 0$) spheres can be written in the form

$$\tilde{\Phi}^{(1)} = \frac{1}{f}(\cosh\eta - \cos\xi)^{1/2}\sum_{n=0}^{\infty}\sum_{m=0}^{n}\exp\left[\left(n+\frac{1}{2}\right)\eta\right] \times P_n^m(\cos\xi)\left[a_{mn}^{(1)}\cos m\varphi + b_{mn}^{(1)}\sin m\varphi\right],$$
$$\tilde{\Phi}^{(2)} = \frac{1}{f}(\cosh\eta - \cos\xi)^{1/2}\sum_{n=0}^{\infty}\sum_{m=0}^{n}\exp\left[-\left(n+\frac{1}{2}\right)\eta\right] \times P_n^m(\cos\xi)\left[a_{mn}^{(2)}\cos m\varphi + b_{mn}^{(2)}\sin m\varphi\right]. \tag{18}$$

In expressions (17) and (18), α_{mn}, β_{mn}, γ_{mn}, δ_{mn} and $a_{mn}^{(1)}$, $b_{mn}^{(1)}$, $a_{mn}^{(2)}$, $b_{mn}^{(2)}$ are unknown coefficients to be determined.

3.1 System of recurrent equations in the case of arbitrary spheres

Equations for unknown coefficients can be obtained with the help of usual boundary conditions on the surface of spheres. Potentials (18) and the total potential $\tilde{\Phi}^{\mathrm{r}} + G_0$ on the surface of each of the nanospheres coincide, which gives the following equations

$$a_{mn}^{(1)}\exp\left[\left(n+\frac{1}{2}\right)\eta_1\right] = \alpha_{mn}\cosh\left[\left(n+\frac{1}{2}\right)\eta_1\right] + \gamma_{mn}\sinh\left[\left(n+\frac{1}{2}\right)\eta_1\right] + c_{mn}\exp\left[-\left(n+\frac{1}{2}\right)|\eta_1-\eta'|\right],$$
$$a_{mn}^{(2)}\exp\left[-\left(n+\frac{1}{2}\right)\eta_2\right] = \alpha_{mn}\cosh\left[\left(n+\frac{1}{2}\right)\eta_2\right] + \gamma_{mn}\sinh\left[\left(n+\frac{1}{2}\right)\eta_2\right] + c_{mn}\exp\left[-\left(n+\frac{1}{2}\right)|\eta_2-\eta'|\right]. \tag{19}$$

Equations for the coefficients $b_{mn}^{(1)}$ and $b_{mn}^{(2)}$ can be obtained from (19) by the substitutions $a_{mn}^{(1)} \to b_{mn}^{(1)}$, $a_{mn}^{(2)} \to b_{mn}^{(2)}$, and $c_{mn} \to d_{mn}$. To simplify further calculations without loss of generality, we consider an atom located in the half-space $z' \geqslant 0$ outside the second sphere ($\eta_2 > \eta' > 0$).

Let the first ($\eta = \eta_1$) and second ($\eta = \eta_2$) spheres have the dielectric constants ε_1 and ε_2, respectively; the dielectric constant of a medium to which the spheres are embedded is set equal to unity. By using the boundary conditions for the normal derivatives of potentials on the surface of each of the spheres, we obtain two more equations for unknown coefficients. By excluding then the coefficients $a_{mn}^{(1)}$ and $a_{mn}^{(2)}$ from these equations with the help of (19), we find equations for the coefficients α_{mn} and γ_{mn}:

$$(n-m)\cosh\left[\left(n-\frac{1}{2}\right)\eta_1\right]\left\{\varepsilon_1 - \tanh\left[\left(n-\frac{1}{2}\right)\eta_1\right]\right\}\alpha_{m\,n-1} - (2n+1)\cosh\eta_1\cosh\left[\left(n+\frac{1}{2}\right)\eta_1\right] \times\left\{\varepsilon_1 - \tanh\left[\left(n+\frac{1}{2}\right)\eta_1\right] + (\varepsilon_1 - 1)\frac{\tanh\eta_1}{2n+1}\right\}\alpha_{mn} + (n+m+1)\cosh\left[\left(n+\frac{3}{2}\right)\eta_1\right] \times\left\{\varepsilon_1 - \tanh\left[\left(n+\frac{3}{2}\right)\eta_1\right]\right\}\alpha_{m\,n+1} + (n-m) \times\sinh\left[\left(n-\frac{1}{2}\right)\eta_1\right]\left\{\varepsilon_1 - \coth\left[\left(n-\frac{1}{2}\right)\eta_1\right]\right\}\gamma_{m\,n-1} -$$

$$
\begin{aligned}
&-(2n+1)\cosh\eta_1\sinh\left[\left(n+\frac{1}{2}\right)\eta_1\right]\\
&\times\left\{\varepsilon_1-\coth\left[\left(n+\frac{1}{2}\right)\eta_1\right]+(\varepsilon_1-1)\frac{\tanh\eta_1}{2n+1}\right\}\gamma_{mn}\\
&+(n+m+1)\sinh\left[\left(n+\frac{3}{2}\right)\eta_1\right]\\
&\times\left\{\varepsilon_1-\coth\left[\left(n+\frac{3}{2}\right)\eta_1\right]\right\}\gamma_{m\,n+1}=-(\varepsilon_1-1)(n-m)\\
&\times\exp\left[\left(n-\frac{1}{2}\right)(\eta_1-\eta')\right]c_{m\,n-1}+(\varepsilon_1-1)(2n+1)\\
&\times\cosh\eta_1\left(1+\frac{\tanh\eta_1}{2n+1}\right)\exp\left[\left(n+\frac{1}{2}\right)(\eta_1-\eta')\right]c_{mn}\\
&-(\varepsilon_1-1)(n+m+1)\exp\left[\left(n+\frac{3}{2}\right)(\eta_1-\eta')\right]c_{m\,n+1}\quad(20)
\end{aligned}
$$

and

$$
\begin{aligned}
&(n-m)\cosh\left[\left(n-\frac{1}{2}\right)\eta_2\right]\left\{\varepsilon_2+\tanh\left[\left(n-\frac{1}{2}\right)\eta_2\right]\right\}\alpha_{m\,n-1}\\
&-(2n+1)\cosh\eta_2\cosh\left[\left(n+\frac{1}{2}\right)\eta_2\right]\\
&\times\left\{\varepsilon_2+\tanh\left[\left(n+\frac{1}{2}\right)\eta_2\right]-(\varepsilon_2-1)\frac{\tanh\eta_2}{2n+1}\right\}\alpha_{mn}\\
&+(n+m+1)\cosh\left[\left(n+\frac{3}{2}\right)\eta_2\right]\\
&\times\left\{\varepsilon_2+\tanh\left[\left(n+\frac{3}{2}\right)\eta_2\right]\right\}\alpha_{m\,n+1}\\
&+(n-m)\sinh\left[\left(n-\frac{1}{2}\right)\eta_2\right]\left\{\varepsilon_2+\coth\left[\left(n-\frac{1}{2}\right)\eta_2\right]\right\}\gamma_{m\,n-1}\\
&-(2n+1)\cosh\eta_2\sinh\left[\left(n+\frac{1}{2}\right)\eta_2\right]\\
&\times\left\{\varepsilon_2+\coth\left[\left(n+\frac{1}{2}\right)\eta_2\right]-(\varepsilon_2-1)\frac{\tanh\eta_2}{2n+1}\right\}\gamma_{mn}\\
&+(n+m+1)\sinh\left[\left(n+\frac{3}{2}\right)\eta_2\right]\\
&\times\left\{\varepsilon_2+\coth\left[\left(n+\frac{3}{2}\right)\eta_2\right]\right\}\gamma_{m\,n+1}=-(\varepsilon_2-1)(n-m)\\
&\times\exp\left[-\left(n-\frac{1}{2}\right)(\eta_2-\eta')\right]c_{m\,n-1}+(\varepsilon_2-1)(2n+1)\\
&\times\cosh\eta_2\left(1-\frac{\tanh\eta_2}{2n+1}\right)\exp\left[-\left(n+\frac{1}{2}\right)(\eta_2-\eta')\right]c_{mn}\\
&-(\varepsilon_2-1)(n+m+1)\exp\left[-\left(n+\frac{3}{2}\right)(\eta_2-\eta')\right]c_{m\,n+1}.\quad(21)
\end{aligned}
$$

Equations for the coefficients β_{mn} and δ_{mn} can be obtained from (20) and (21) by making the substitutions $\alpha_{mn}\to\beta_{mn}$, $\gamma_{mn}\to\delta_{mn}$, and $c_{mn}\to d_{mn}$.

Recurrent equations (20) and (21) are constructed so that for the specified index $m=m'$ the infinite system of equation appears with $n\geqslant m'$ for unknown coefficients. It follows from the structure of Eqns (20) and (21) that for the large values of the index $n\gg 1$, the coefficients α_{mn} and γ_{mn} will tend to zero. This allows the replacement of the infinite system of equations by a finite system with $m\leqslant n\leqslant N$, where N is chosen in accordance with the specified accuracy.

3.2 Solution in the case of a cluster of two ideally conducting nanospheres

In the case of ideally conducting spheres, we can obtain the following explicit expressions for the coefficients α_{mn}, β_{mn}, and γ_{mn}, δ_{mn} [27]

$$
\begin{aligned}
&\begin{pmatrix}\alpha^{\mathrm{ic}}_{mn}\\ \beta^{\mathrm{ic}}_{mn}\end{pmatrix}=-\begin{pmatrix}c_{mn}\\ d_{mn}\end{pmatrix}\left\{\exp\left[\left(n+\frac{1}{2}\right)(\eta_1-\eta')\right]\right.\\
&\times\sinh\left[\left(n+\frac{1}{2}\right)\eta_2\right]-\exp\left[-\left(n+\frac{1}{2}\right)(\eta_2-\eta')\right]\\
&\left.\times\sinh\left[\left(n+\frac{1}{2}\right)\eta_1\right]\right\}\left\{\sinh\left[\left(n+\frac{1}{2}\right)(\eta_2-\eta_1)\right]\right\}^{-1}\\
&-\delta(m,0)\begin{pmatrix}1\\0\end{pmatrix}\left\{A_1\exp\left[\left(n+\frac{1}{2}\right)\eta_1\right]\sinh\left[\left(n+\frac{1}{2}\right)\eta_2\right]\right.\\
&\left.-A_2\exp\left[-\left(n+\frac{1}{2}\right)\eta_2\right]\sinh\left[\left(n+\frac{1}{2}\right)\eta_1\right]\right\}\\
&\times\left\{\sinh\left[\left(n+\frac{1}{2}\right)(\eta_2-\eta_1)\right]\right\}^{-1},\qquad(22)
\end{aligned}
$$

and

$$
\begin{aligned}
&\begin{pmatrix}\gamma^{\mathrm{ic}}_{mn}\\ \delta^{\mathrm{ic}}_{mn}\end{pmatrix}=\begin{pmatrix}c_{mn}\\ d_{mn}\end{pmatrix}\left\{\exp\left[\left(n+\frac{1}{2}\right)(\eta_1-\eta')\right]\right.\\
&\times\cosh\left[\left(n+\frac{1}{2}\right)\eta_2\right]-\exp\left[-\left(n+\frac{1}{2}\right)(\eta_2-\eta')\right]\\
&\left.\times\cosh\left[\left(n+\frac{1}{2}\right)\eta_1\right]\right\}\left\{\sinh\left[\left(n+\frac{1}{2}\right)(\eta_2-\eta_1)\right]\right\}^{-1}\\
&+\delta(m,0)\begin{pmatrix}1\\0\end{pmatrix}\left\{A_1\exp\left[\left(n+\frac{1}{2}\right)\eta_1\right]\cosh\left[\left(n+\frac{1}{2}\right)\eta_2\right]\right.\\
&\left.-A_2\exp\left[-\left(n+\frac{1}{2}\right)\eta_2\right]\cosh\left[\left(n+\frac{1}{2}\right)\eta_1\right]\right\}\\
&\times\left\{\sinh\left[\left(n+\frac{1}{2}\right)(\eta_2-\eta_1)\right]\right\}^{-1},\qquad(23)
\end{aligned}
$$

where

$$
A_1=-\frac{(C_{22}+C_{21})B_1+C_{12}B_2}{C_{12}C_{22}+C_{21}C_{11}+C_{11}C_{22}};
$$

$$A_2 = -\frac{C_{21}B_1 + (C_{11}+C_{12})B_2}{C_{12}C_{22} + C_{21}C_{11} + C_{11}C_{22}};$$

$$B_1 = 2\sum_{n=0}^{\infty} c_{0n}\left\{\sinh\left[\left(n+\frac{1}{2}\right)(\eta_2-\eta')\right]\right.$$
$$\left.\times\left\{\sinh\left[\left(n+\frac{1}{2}\right)(\eta_2-\eta_1)\right]\right\}^{-1}\right\}\exp\left[\left(n+\frac{1}{2}\right)\eta_1\right];$$

$$B_2 = 2\sum_{n=0}^{\infty} c_{0n}\left\{\sinh\left[\left(n+\frac{1}{2}\right)(\eta'-\eta_1)\right]\right.$$
$$\left.\times\left\{\sinh\left[\left(n+\frac{1}{2}\right)(\eta_2-\eta_1)\right]\right\}^{-1}\right\}\exp\left[-\left(n+\frac{1}{2}\right)\eta_2\right];$$

$$C_{11} = 2\sum_{n=0}^{\infty}\left\{\sinh\left[\left(n+\frac{1}{2}\right)\eta_2\right]\right.$$
$$\left.\times\left\{\sinh\left[\left(n+\frac{1}{2}\right)(\eta_2-\eta_1)\right]\right\}^{-1}\right\}\exp\left[\left(n+\frac{1}{2}\right)\eta_1\right];$$

$$C_{12} = C_{21} = \sum_{n=0}^{\infty}\exp\left[-\left(n+\frac{1}{2}\right)(\eta_2-\eta_1)\right]$$
$$\times\left\{\sinh\left[\left(n+\frac{1}{2}\right)(\eta_2-\eta_1)\right]\right\}^{-1}; \qquad (25)$$

$$C_{22} = -2\sum_{n=0}^{\infty}\left\{\sinh\left[\left(n+\frac{1}{2}\right)\eta_1\right]\right.$$
$$\left.\times\left\{\sinh\left[\left(n+\frac{1}{2}\right)(\eta_2-\eta_1)\right]\right\}^{-1}\right\}\exp\left[-\left(n+\frac{1}{2}\right)\eta_2\right].$$

The results of analysis of expressions (22)–(25) will be presented below.

4. Natural oscillations in a two-nanosphere cluster

To study the influence of a cluster on the optical properties of atoms and molecules, it is necessary to know the properties of its natural oscillations. The natural oscillations of a cluster (and generally speaking, of any system) are possible only for some (negative) values of the dielectric constant of the cluster material. To find the resonance values of the dielectric constant, it is necessary to solve the homogeneous variant of the system of equations (20), (21) with $c_{mn} = 0$, by considering the dielectric constant as the eigenvalue. In the case of a cluster of two identical spheres ($R_1 = R_2 = R_0$, $-\eta_1 = \eta_2 = \eta_0$), the system of recurrent equations (20) and (21) can be represented in the form of two independent system of equations for each of the coefficients α_{mn} (β_{mn}) and γ_{mn} (δ_{mn}). We will call the modes excited by a homogeneous electric field directed along the symmetry axis of the cluster (longitudinal modes) the L modes. The modes observed upon excitation by a homogeneous field directed perpendicular to the axis (transverse modes) will be called the T modes. The resonance values of the dielectric constant and the corresponding frequencies of the L and T modes can be found, for example, within the framework of the method of hybridisation of plasmon oscillations of individual spheres [20]. A two-nanosphere cluster can also exhibit the M modes [21], which are not efficiently excited by a plane wave and have a noticeably smaller effective volume than the L and T modes.

Figure 3 presents the dependences of the resonance dielectric constant ε_{mn} on the distance between identical nanospheres for $m = 0$ and 1. One can see that, as the distance between nanospheres is increased, the resonance dielectric constants corresponding to the T and L modes tends to the well-known values $-(n+1)/n$ ($n = 1, 2, 3, \ldots$) [23, 24], which correspond to the modes of different multipolarities excited in a sphere. As for the M modes, they can exist only under the condition $R_{12}(2R_0)^{-1} \leqslant 1.2$. These modes appear due to the formation of the bound two-plasmon state, as upon formation of molecules from atoms approaching each other.

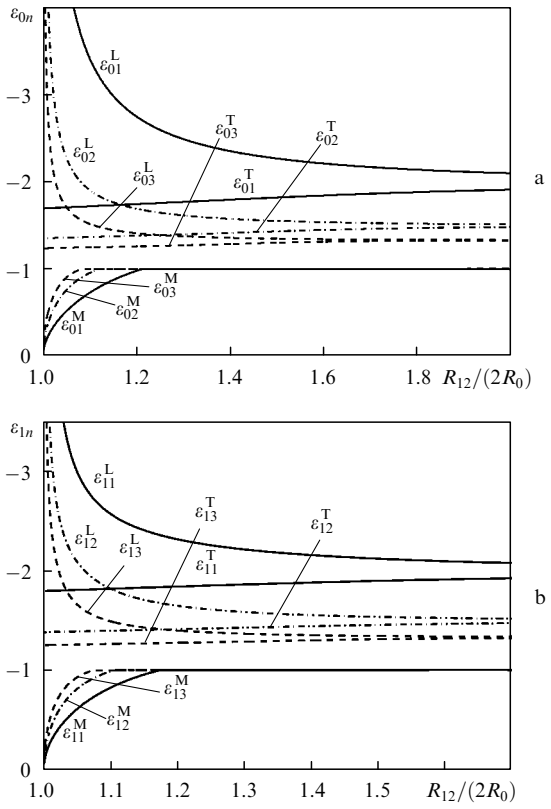

Figure 3. Resonance dielectric constant ε_{mn} for the L, T and M modes as a function of the normalised distance $R_{12}/(2R_0)$ between two identical nanospheres for $m = 0$ (a) and 1 (b).

Figure 3 also shows that the behaviour of the spectra in the region of almost touching spheres becomes very complex. Nevertheless, in this case the asymptotic solutions can be found for the resonance dielectric constant ε_{mn}. We have for the M modes

$$\varepsilon_{mn}^{M} = -(n+m+\delta_m)\eta_0 + \ldots, \qquad (26)$$

where $n = 1, 2, 3, \ldots$; $m = 0, 1, 2, \ldots$; $\delta_0 = 1/2$, $\delta_1 \approx -0.086, \ldots$. The analytic solution for the L modes has the form

$$\varepsilon_{mn}^{L} = -(n+m-1/2)^{-1}\eta_0^{-1} + \ldots, \qquad (27)$$

where $n = 1, 2, 3, \ldots$; $m = 0, 1, 2, 3$. In the case of the T modes, we failed to obtain the analytic solution. Let us present several first values of the resonance dielectric constant:

$$\varepsilon_{01}^{\mathrm{T}} \approx -1.696, \quad \varepsilon_{02}^{\mathrm{T}} \approx -1.355, \quad \varepsilon_{03}^{\mathrm{T}} \approx -1.237,$$
$$\varepsilon_{11}^{\mathrm{T}} \approx -1.799, \quad \varepsilon_{12}^{\mathrm{T}} \approx -1.386, \quad \varepsilon_{13}^{\mathrm{T}} \approx -1.182. \tag{28}$$

The eigenvectors of the M and L modes corresponding to the resonance dielectric constants (26) and (27) can be calculated analytically in the limit of closely spaced spheres:

$$\alpha_{0n}^{\mathrm{M}} = \begin{cases} -\dfrac{1}{\mathscr{M}\cosh[(n+1/2)\eta_0]}, & n \leqslant \mathscr{M}-1, \\ \dfrac{1}{\cosh[(\mathscr{M}+1/2)\eta_0]}, & n = \mathscr{M}, \\ 0, & n > \mathscr{M}, \end{cases}$$
$$\gamma_{mn}^{\mathrm{L}} = \frac{\delta(n-m+1,\mathscr{L})}{\sinh[(\mathscr{L}+m-1/2)\eta_0]}, \tag{29}$$

where $\mathscr{M}$ and $\mathscr{L}$ are the numbers of the M and L modes; $\mathscr{M}, \mathscr{L} = 1, 2, 3, \ldots$; $m, n = 0, 1, 2, \ldots$. Note that the similar expression for δ_{mn}^{L} coincides with expression (29) for δ_{mn}^{L}, while $\beta_{0n}^{\mathrm{M}} = 0$. To these vectors, the expressions for the eigenfunctions of the potential correspond, which are obtained by substituting (29) into (17) and (18). The eigenfunctions of the axially symmetric M mode ($m = 0$) in the space between spheres have the form

$$\tilde{\Phi}_{0\mathscr{M}}\big|_{\eta_0\to 0} \approx -\frac{1}{\mathscr{M}f}(\cosh\eta - \cos\xi)^{1/2}$$
$$\times \sum_{n=0}^{\mathscr{M}-1} \frac{\cosh[(n+1/2)\eta]}{\cosh[(n+1/2)\eta_0]} P_n(\cos\xi) + \frac{1}{f}(\cosh\eta - \cos\xi)^{1/2}$$
$$\times \frac{\cosh[(\mathscr{M}+1/2)\eta]}{\cosh[(\mathscr{M}+1/2)\eta_0]} P_{\mathscr{M}}(\cos\xi). \tag{30}$$

The eigenfunctions inside the first sphere are described by the expression

$$\tilde{\Phi}_{0\mathscr{M}}^{(1)}\big|_{\eta_0\to 0} \approx -\frac{1}{\mathscr{M}f}(\cosh\eta - \cos\xi)^{1/2}$$
$$\times \sum_{n=0}^{\mathscr{M}-1} \exp\left[\left(n+\frac{1}{2}\right)(\eta+\eta_0)\right] P_n(\cos\xi) \tag{31}$$
$$+ \frac{1}{f}(\cosh\eta - \cos\xi)^{1/2} \exp\left[\left(\mathscr{M}+\frac{1}{2}\right)(\eta+\eta_0)\right] P_{\mathscr{M}}(\cos\xi).$$

The eigenfunctions inside the second sphere are described by a similar expression.

The eigenfunctions of the L mode in the space between spheres and inside the first sphere are described by the expressions

$$\tilde{\Phi}_{m\mathscr{L}}\big|_{\eta_0\to 0} \approx \frac{1}{f}(\cosh\eta - \cos\xi)^{1/2}$$
$$\times \frac{\sinh[(\mathscr{L}+m-1/2)\eta]}{\sinh[(\mathscr{L}+m-1/2)\eta_0]} P_{\mathscr{L}+m-1}^{m}(\cos\xi)\cos m\varphi, \tag{32}$$

$$\tilde{\Phi}_{m\mathscr{L}}^{(1)}\big|_{\eta_0\to 0} \approx -\frac{1}{f}(\cosh\eta - \cos\xi)^{1/2}$$
$$\times \exp\left[\left(\mathscr{L}+m-\frac{1}{2}\right)(\eta+\eta_0)\right] P_{\mathscr{L}+m-1}^{m}(\cos\xi)\cos m\varphi, \tag{33}$$

respectively. The eigenfunctions inside the second sphere are described by similar expressions.

5. Spontaneous decay rate of the excited state of an atom near a two-nanosphere cluster

As follows from the general theory presented in section 2, the spontaneous decay rate near a nanobody has the radiative and nonradiative components [see expression (7)]. In this section, we will discuss separately both the radiative and nonradiative components of the decay rate.

5.1 General expression for the radiative component of the spontaneous decay rate

It follows from (8) that to find the radiative component of the spontaneous decay rate, it is necessary to calculate the total dipole moment of the atom + two nanospheres system. To find the dipole moment, we obtain the asymptotics of potential (17) at large distances between an atom and a cluster and compare it with the known expression for the potential of a dipole at large distances $(\boldsymbol{d}_{\mathrm{tot}}\boldsymbol{R})/R^3$.

Let R, ϑ, and φ be the coordinates of the spherical system. Then, with an accuracy to the terms of the second-order smallness ($R \to \infty$), the expressions for the coordinates of the bispherical system will take the form $\eta \approx 2(f/R)\cos\vartheta$ and $\xi \approx 2(f/R)\sin\vartheta$. By substituting these expressions into (17), expanding the obtained expression in a small parameter f/R ($f/R \ll 1$), and comparing it with the potential of a dipole at large distances, we find the relations for the induced dipole moment of the two-nanosphere cluster:

$$\delta d_x = -\sqrt{2}\, f(\boldsymbol{d}_0\nabla') \sum_{n=1}^{\infty} n(n+1)\alpha_{1n},$$
$$\delta d_y = -\sqrt{2}\, f(\boldsymbol{d}_0\nabla') \sum_{n=1}^{\infty} n(n+1)\beta_{1n}, \tag{34}$$
$$\delta d_z = 2\sqrt{2}\, f(\boldsymbol{d}_0\nabla') \sum_{n=0}^{\infty} (n+1/2)\gamma_{0n}.$$

Thus, it follows from (34) that to find the induced dipole moment, it is necessary to calculate the corresponding derivatives from coefficients α_{1n}, β_{1n}, and γ_{0n}. By knowing these derivatives, we find from (8) the radiative component of the spontaneous decay rate of the excited state of an atom located near a cluster of two nanospheres made of an arbitrary material and having different radii.

5.2 General expression for the nonradiative component of the spontaneous decay rate

By using expression (7), we can find the principal term in the expression for the nonradiative component of the spontaneous decay rate of the excited state of an atom near a two-nanosphere cluster, which is determined by the contribution of the reflected field in the quasi-static approximation. For this purpose, it is necessary to differ-

entiate properly (17). As a result, we obtain the following expressions for the nonradiative component of the decay rate of the excited state of the atom near the two-nanosphere cluster for the characteristic directions of the dipole moment of the atom ($\varphi' = 0$).

The dipole moment of the atom is oriented along the x axis ($\boldsymbol{d}_0 = d_0\boldsymbol{e}_x$):

$$\left(\frac{\gamma}{\gamma_0}\right)_x^{\text{nrad}} = -\frac{3(\cosh\eta' - \cos\xi')^{1/2}}{2(k_0 f)^3}$$

$$\times \operatorname{Im}\left\{\frac{1}{2}\sinh\eta'\cosh\eta'\sin^2\xi'\right.$$

$$\times \sum_{n=0}^{\infty}\sum_{m=0}^{n}\left\{\frac{\partial\alpha_{mn}}{\partial\eta'}\cosh\left[\left(n+\frac{1}{2}\right)\eta'\right]\right.$$

$$\left.+\frac{\partial\gamma_{mn}}{\partial\eta'}\sinh\left[\left(n+\frac{1}{2}\right)\eta'\right]\right\}P_n^m(\cos\xi')$$

$$-\frac{1}{2}\cosh\eta'\sin\xi'(\cosh\eta'\cos\xi'-1)$$

$$\times \sum_{n=0}^{\infty}\sum_{m=0}^{n}\left\{\frac{\partial\alpha_{mn}}{\partial\xi'}\cosh\left[\left(n+\frac{1}{2}\right)\eta'\right]\right.$$

$$\left.+\frac{\partial\gamma_{mn}}{\partial\eta'}\sinh\left[\left(n+\frac{1}{2}\right)\eta'\right]\right\}P_n^m(\cos\xi') + \sinh^2\eta'\sin^2\xi'$$

$$\times \sum_{n=0}^{\infty}\sum_{m=0}^{n}\left(n+\frac{1}{2}\right)\left\{\frac{\partial\alpha_{mn}}{\partial\eta'}\sinh\left[\left(n+\frac{1}{2}\right)\eta'\right]\right.$$

$$\left.+\frac{\partial\gamma_{mn}}{\partial\eta'}\cosh\left[\left(n+\frac{1}{2}\right)\eta'\right]\right\}P_n^m(\cos\xi')$$

$$-\sinh\eta'\sin\xi'(\cosh\eta'\cos\xi'-1)$$

$$\times \sum_{n=0}^{\infty}\sum_{m=0}^{n}\left(n+\frac{1}{2}\right)\left\{\frac{\partial\alpha_{mn}}{\partial\xi'}\sinh\left[\left(n+\frac{1}{2}\right)\eta'\right]\right.$$

$$\left.+\frac{\partial\gamma_{mn}}{\partial\xi'}\cosh\left[\left(n+\frac{1}{2}\right)\eta'\right]\right\}P_n^m(\cos\xi')$$

$$-\sinh\eta'\sin\xi'(\cosh\eta'\cos\xi'-1)$$

$$\times \sum_{n=0}^{\infty}\sum_{m=0}^{n}\left\{\frac{\partial\alpha_{mn}}{\partial\eta'}\cosh\left[\left(n+\frac{1}{2}\right)\eta'\right]\right.$$

$$\left.+\frac{\partial\gamma_{mn}}{\partial\eta'}\sinh\left[\left(n+\frac{1}{2}\right)\eta'\right]\right\}\frac{\partial P_n^m(\cos\xi')}{\partial\xi'}$$

$$+(\cosh\eta'\cos\xi'-1)^2\sum_{n=0}^{\infty}\sum_{m=0}^{n}\left\{\frac{\partial\alpha_{mn}}{\partial\xi'}\cosh\left[\left(n+\frac{1}{2}\right)\eta'\right]\right.$$

$$\left.+\frac{\partial\gamma_{mn}}{\partial\xi'}\sinh\left[\left(n+\frac{1}{2}\right)\eta'\right]\right\}\frac{\partial P_n^m(\cos\xi')}{\partial\xi'}\Bigg\}. \tag{35}$$

The dipole moment of the atom is oriented along the y axis ($\boldsymbol{d}_0 = d_0\boldsymbol{e}_y$):

$$\left(\frac{\gamma}{\gamma_0}\right)_y^{\text{nrad}} = -\frac{3}{2(k_0 f)^3}\frac{(\cosh\eta' - \cos\xi')^{5/2}}{\sin^2\xi'}$$

$$\times \operatorname{Im}\left\{\sum_{n=1}^{\infty}\sum_{m=1}^{n} m\left\{\left.\frac{\partial\beta_{mn}}{\partial\varphi'}\right|_{\varphi'=0}\cosh\left[\left(n+\frac{1}{2}\right)\eta'\right] + \left.\frac{\partial\delta_{mn}}{\partial\varphi'}\right|_{\varphi'=0}\right.\right.$$

$$\left.\left.\times\sinh\left[\left(n+\frac{1}{2}\right)\eta'\right]\right\}P_n^m(\cos\xi')\right\}. \tag{36}$$

The dipole moment of the atom is oriented along the z axis ($\boldsymbol{d}_0 = d_0\boldsymbol{e}_z$):

$$\left(\frac{\gamma}{\gamma_0}\right)_z^{\text{nrad}} = -\frac{3(\cosh\eta' - \cos\xi')^{1/2}}{2(k_0 f)^3}$$

$$\times \operatorname{Im}\left\{\frac{1}{2}\sinh\eta'\cos\xi'(\cosh\eta'\cos\xi'-1)\right.$$

$$\times \sum_{n=0}^{\infty}\sum_{m=0}^{n}\left\{\frac{\partial\alpha_{mn}}{\partial\eta'}\cosh\left[\left(n+\frac{1}{2}\right)\eta'\right]\right.$$

$$\left.+\frac{\partial\gamma_{mn}}{\partial\eta'}\sinh\left[\left(n+\frac{1}{2}\right)\eta'\right]\right\}P_n^m(\cos\xi')$$

$$+\frac{1}{2}\sinh^2\eta'\sin\xi'\cos\xi'$$

$$\times \sum_{n=0}^{\infty}\sum_{m=0}^{n}\left\{\frac{\partial\alpha_{mn}}{\partial\xi'}\cosh\left[\left(n+\frac{1}{2}\right)\eta'\right]\right.$$

$$\left.+\frac{\partial\gamma_{mn}}{\partial\xi'}\sinh\left[\left(n+\frac{1}{2}\right)\eta'\right]\right\}P_n^m(\cos\xi') + (\cosh\eta'\cos\xi'-1)^2$$

$$\times \sum_{n=0}^{\infty}\sum_{m=0}^{n}\left(n+\frac{1}{2}\right)\left\{\frac{\partial\alpha_{mn}}{\partial\eta'}\sinh\left[\left(n+\frac{1}{2}\right)\eta'\right]\right.$$

$$\left.+\frac{\partial\gamma_{mn}}{\partial\eta'}\cosh\left[\left(n+\frac{1}{2}\right)\eta'\right]\right\}P_n^m(\cos\xi')$$

$$+\sinh\eta'\sin\xi'(\cosh\eta'\cos\xi'-1)$$

$$\times \sum_{n=0}^{\infty}\sum_{m=0}^{n}\left(n+\frac{1}{2}\right)\left\{\frac{\partial\alpha_{mn}}{\partial\xi'}\sinh\left[\left(n+\frac{1}{2}\right)\eta'\right]\right.$$

$$\left.+\frac{\partial\gamma_{mn}}{\partial\xi'}\cosh\left[\left(n+\frac{1}{2}\right)\eta'\right]\right\}P_n^m(\cos\xi')$$

$$+\sinh\eta'\sin\xi'(\cosh\eta'\cos\xi'-1)$$

$$\times \sum_{n=0}^{\infty}\sum_{m=0}^{n}\left\{\frac{\partial\alpha_{mn}}{\partial\eta'}\cosh\left[\left(n+\frac{1}{2}\right)\eta'\right]\right.$$

$$\left.+\frac{\partial\gamma_{mn}}{\partial\eta'}\sinh\left[\left(n+\frac{1}{2}\right)\eta'\right]\right\}\frac{\partial P_n^m(\cos\xi')}{\partial\xi'} + \sinh^2\eta'\sin^2\xi'$$

$$\times \sum_{n=0}^{\infty}\sum_{m=0}^{n}\left\{\frac{\partial\alpha_{mn}}{\partial\xi'}\cosh\left[\left(n+\frac{1}{2}\right)\eta'\right]+\right.$$

$$+\frac{\partial\gamma_{mn}}{\partial\xi'}\sinh\left[\left(n+\frac{1}{2}\right)\eta'\right]\Bigg\}\frac{\partial P_n^m(\cos\xi')}{\partial\xi'}\Bigg\}. \tag{37}$$

As follows from expressions (35)–(37), to find the nonradiative component of the spontaneous decay rate of the excited state of the atom near the two-nanosphere cluster, it is necessary to calculate the corresponding derivatives from the coefficients α_{nm}, β_{nm}, and γ_{nm}, δ_{nm} by solving the system of equations obtained by differentiating (20) and (21) with respect to the corresponding coordinate. In this case, both indices m and n take all the values from 0 to N, which results in a considerable increase in the number of systems to be solved compared to the number of systems of equations for the radiative component of the spontaneous decay rate, where equations only with two indices $m = 0$ and 1 are used. Nevertheless, because the required coefficients vanish for $n < m$, the number of equations in the systems to be solved with the specified accuracy and the specified position of an atom decreases with increasing m, which provides a comparatively short time of computer calculations. Note also that, when an atom is located on the polar axis ($\xi' = 0$ or π), the derivatives from coefficients can be calculated by solving only two systems of equations with indices $m = 0$ and 1 because Legendre function and their derivatives used in expressions (35)–(37) vanish at the axis for all $m > 1$.

However, to achieve the required accuracy of calculations when an atom approaches the surface of one of the nanospheres, it is necessary to solve systems with the increasing number N of equations. Therefore, when the atom is located close to the surface, there is no point in using expressions (35)–(37) for determining the nonradiative component of the decay rate (and the frequency shift). On the other hand, for small distances of the atom from the nanosphere surface, it can be well approximated by a plane. This approximation allows us to find the principal terms in expressions describing contributions to the nonradiative component of the spontaneous decay rate of the excited state of the atom. Let the atom be located in a medium with the dielectric constant equal to unity near a plane interface with a medium with the dielectric constant ε. In this case, the solution for the nonradiative component of the decay rate is well known and has the form

$$\left(\frac{\gamma}{\gamma_0}\right)_{\text{tang}}^{\text{nrad}}=\frac{3}{16(k_0\Delta)^3}\,\text{Im}\,\frac{\varepsilon-1}{\varepsilon+1},$$
$$\left(\frac{\gamma}{\gamma_0}\right)_{\text{norm}}^{\text{nrad}}=2\left(\frac{\gamma}{\gamma_0}\right)_{\text{tang}}^{\text{nrad}} \tag{38}$$

for the tangential and radial (normal) orientations of the dipole moment of the atom, respectively, where Δ is the distance from the interface to the atom. Expression (38) is valid for an atom located outside the cluster. If an atom is located between spheres, the principal term of the contribution to the nonradiative component of the decay rate is calculated similarly by replacing spherical surfaces by planes. In the given case, an atom will be located in the medium with the dielectric constant $\varepsilon = 1$ between two semi-infinite media with dielectric constants ε_1 and ε_2. The nonradiative component of the decay rate for such an atom is described by the following expressions:

The dipole moment of the atom is oriented tangentially with respect to the sphere surface:

$$\left(\frac{\gamma}{\gamma_0}\right)_{\text{tang}}^{\text{nrad}}=\frac{3}{128k_0^3}\,\text{Im}\Bigg\{\beta_2\sum_{n=0}^{\infty}(\beta_1\beta_2)^n$$
$$\times\left\{\frac{8}{[2(n+1/2)z_0-z']^3}-\frac{\beta_1}{(n+1)^3z_0^3}\right\}\Bigg\}+\frac{3}{128k_0^3} \tag{39}$$
$$\times\,\text{Im}\Bigg\{\beta_1\sum_{n=0}^{\infty}(\beta_1\beta_2)^n\left\{\frac{8}{[2(n+1/2)z_0+z']^3}-\frac{\beta_2}{(n+1)^3z_0^3}\right\}\Bigg\}.$$

The dipole moment of the atom is oriented normally to the sphere surface:

$$\left(\frac{\gamma}{\gamma_0}\right)_{\text{norm}}^{\text{nrad}}=\frac{3}{64k_0^3}\,\text{Im}\Bigg\{\beta_2\sum_{n=0}^{\infty}(\beta_1\beta_2)^n$$
$$\times\left\{\frac{8}{[2(n+1/2)z_0-z']^3}+\frac{\beta_1}{(n+1)^3z_0^3}\right\}\Bigg\}+\frac{3}{64k_0^3} \tag{40}$$
$$\times\,\text{Im}\Bigg\{\beta_1\sum_{n=0}^{\infty}(\beta_1\beta_2)^n\left\{\frac{8}{[2(n+1/2)z_0+z']^3}+\frac{\beta_2}{(n+1)^3z_0^3}\right\}\Bigg\}.$$

In expressions (39) and (40)

$$\beta_1=\frac{\varepsilon_1-1}{\varepsilon_1+1};\quad \beta_2=\frac{\varepsilon_2-1}{\varepsilon_2+1};$$

z' is the coordinate of the atom measured from the gap middle; and $2z_0$ is the distance between the boundaries of media.

5.3 Spontaneous decay rate in the case of ideally conducting nanospheres

Although the quasi-static problem in this case has the explicit solution, the general expressions for the decay rate are too cumbersome. Therefore, we consider below a particular case of two identical ideally conducting nanospheres ($-\eta_1 = \eta_2 = \eta_0$).

5.3.1 General expressions for the spontaneous decay rate of the excited state of an atom near a cluster of two identical ideally conducting nanospheres

In the case of ideally conducting nanospheres, we can use expressions (22) and (23) and obtain from (34) explicit expressions for the induced dipole moment

$$\delta d_x=2\sqrt{2}f(\boldsymbol{d}_0\nabla')\sum_{n=1}^{\infty}n(n+1)c_{1n}$$
$$\times\frac{\cosh[(n+1/2)\eta']}{\exp[(2n+1)\eta_0]+1},$$
$$\delta d_y=2\sqrt{2}f(\boldsymbol{d}_0\nabla')\sum_{n=1}^{\infty}n(n+1)d_{1n}$$
$$\times\frac{\cosh[(n+1/2)\eta']}{\exp[(2n+1)\eta_0]+1}, \tag{41}$$
$$\delta d_z=-4\sqrt{2}f(\boldsymbol{d}_0\nabla')\sum_{n=0}^{\infty}(n+1/2)c_{0n}$$
$$\times\frac{\sinh[(n+1/2)\eta']}{\exp[(2n+1)\eta_0]-1}+2\sqrt{2}f(\boldsymbol{d}_0\nabla')(A_1-A_2)\times$$

$$\times \sum_{n=0}^{\infty} \frac{n+1/2}{\exp[(2n+1)\eta_0]-1},$$

where

$$A_1 - A_2 = \frac{4}{2C_{12}+C_{11}} \sum_{n=0}^{\infty} c_{0n} \frac{\sinh[(n+1/2)\eta']}{\exp[(2n+1)\eta_0]-1}; \quad (42)$$

$$C_{11} = \sum_{n=0}^{\infty} \frac{2}{\exp[(2n+1)\eta_0]+1};$$
$$C_{12} = \sum_{n=0}^{\infty} \frac{2}{\exp[2(2n+1)\eta_0]-1}. \quad (43)$$

Then, by using expression (8), we find the explicit expression for the spontaneous decay rate (nonradiative decay in the case of ideally conducting nanobodies is absent).

5.3.2 Asymptotic expressions for the spontaneous decay rate at small distances between spheres

Despite the explicit form of expressions for the induced dipole moment (41), their study is a separate problem. Nevertheless, in the most interesting case of closely spaced nanospheres, it is possible to find simple asymptotic expressions for the induced dipole moment and decay rate.

Atom is located at the cluster centre

Of special interest is a symmetric problem, i.e. the case when an atom is located midway between two identical spheres ($\eta' = 0$ and $\xi' = \pi$). Without loss of generality, we can assume that $\varphi' = 0$ and consider two cases of the orientation of the dipole momentum of the atom.

The dipole moment is oriented along the x axis ($\boldsymbol{d}_0 = d_0 \boldsymbol{e}_x$). The induced dipole moment can be found from expressions (41). By using the Watson transformation of a slowly converging series ($\eta_0 \to 0$) to a rapidly converging series, we obtain the expression ($\delta d_y = \delta d_z = 0$) [27]:

$$\frac{\delta d_x}{d_0} = -1 + \frac{\pi}{\eta_0} \sum_{k=0}^{\infty} \left[1 + \frac{\pi^2}{\eta_0^2}(2k+1)^2\right] \times \left\{\cosh\left[\frac{\pi^2}{2\eta_0^2}(2k+1)\right]\right\}^{-1}. \quad (44)$$

By retaining several first terms in (44), we obtain good asymptotics in the region of small η_0

$$\frac{\delta d_x}{d_0} = -1 + \frac{2\pi^3}{\eta_0^3} \exp\left(-\frac{\pi^2}{2\eta_0}\right) + \dots. \quad (45)$$

Thus, when the distance between nanospheres is small enough, the spontaneous decay rate of an atom located between them, which has the dipole moment directed perpendicular to the axis connecting the centres of spheres, is close to zero because the dipole moment induced on spheres compensates completely for the dipole moment of the atom.

The dipole moment is oriented along the z axis ($\boldsymbol{d}_0 = d_0 \boldsymbol{e}_z$). In this case, by using the Watson transformation, we obtain from (41) the expression ($\delta d_x = \delta d_y = 0$) [27]

$$\frac{\delta d_z}{d_0} = -1 + \frac{8\pi^3}{\eta_0^3} \sum_{k=1}^{\infty} \frac{k^2}{\cosh(\pi^2 k/\eta_0)} + \frac{2\sqrt{2}f}{d_0} (\boldsymbol{d}_0\nabla')(A_1 - A_2) \sum_{n=0}^{\infty} \frac{n+1/2}{\exp[(2n+1)\eta_0]-1}, \quad (46)$$

where

$$(\boldsymbol{d}_0\nabla')(A_1 - A_2) = \frac{8\sqrt{2}\, d_0}{(C_{11}+2C_{12})f} \times \sum_{n=0}^{\infty} (-1)^n \frac{n+1/2}{\exp[(2n+1)\eta_0]-1}.$$

Series remaining in (46) can be summed in the case of small η_0 by using the Mellin transformation; the application of this transformation for calculating the asymptotics of series is described in detail in [42]. As a result, we obtain the asymptotics ($\eta_0 \to 0$):

$$\frac{\delta d_z}{d_0} \approx -1 + \frac{16\pi^3}{\eta_0^3}\left[\exp\left(-\frac{\pi^2}{\eta_0}\right) + 4\exp\left(-\frac{2\pi^2}{\eta_0}\right) + \dots\right] + \frac{2\zeta(2)}{[\gamma_E + \ln(2/\eta_0)]\eta_0^2} - \frac{1}{6[\gamma_E + \ln(2/\eta_0)]} \times \left\{1 + \zeta(2) + \frac{\zeta(2)}{6[\gamma_E + \ln(2/\eta_0)]}\right\} + \frac{1}{\gamma_E + \ln(2/\eta_0)} \times \left\{\frac{1}{72}[\zeta(2) - 1] + \frac{1}{\gamma_E + \ln(2/\eta_0)} \times \left\{\frac{1}{432} + \frac{43}{21600}\zeta(2) + \frac{\zeta(2)}{2592[\gamma_E + \ln(2/\eta_0)]}\right\}\right\}\eta_0^2 + \dots. \quad (47)$$

Here, ζ is the Riemann zeta function; $\gamma_E \approx 0.577216$ is the Euler constant. Thus, the spontaneous decay rate of an atom, located exactly between spheres and having the dipole moment directed along the line connecting the centres of spheres, infinitely increases as nanospheres come closer together.

Atom is located on the surface of one of the nanospheres

The case of the tangential orientation of the dipole moment with respect to the surface is trivial: the decay rates of the excited state of the atom vanish due to the boundary conditions. This is explained by the fact that the dipole moment induced on spheres is equal to the dipole moment of the atom.

The case of the normal orientation of the dipole with respect to the sphere surface ($\boldsymbol{d}_0 = d_0 \boldsymbol{e}_z$) is more complex, and we consider only situations when the atom is located at the surface points remotest from ($\xi' \to 0$) or closest to ($\xi' = \pi$) the system centre. Without loss of generality, we assume that $\varphi' = 0$.

The induced dipole moment of an atom located at the sphere-surface point remotest from the centre ($\xi' \to 0$) has the form

$$\frac{\delta d_z}{d_0} = 2 + \cosh\eta_0 + 16\sinh^3\left(\frac{\eta_0}{2}\right) \sum_{n=0}^{\infty} \left(n + \frac{1}{2}\right)^2 \times \frac{\exp[-(n+1/2)\eta_0]}{\exp[(2n+1)\eta_0]-1} + \frac{2\sqrt{2}f}{d_0}(\boldsymbol{d}_0\nabla')(A_1 - A_2) \times \sum_{n=0}^{\infty} \frac{n+1/2}{\exp[(2n+1)\eta_0]-1}, \quad (48)$$

where

$$(\boldsymbol{d}_0\nabla')(A_1 - A_2) = -\frac{\sqrt{2}\,d_0}{(C_{11}+2C_{12})f} \times\left\{\sinh\eta_0 + 8\sinh^3\left(\frac{\eta_0}{2}\right) \times\sum_{n=0}^{\infty}\left(n+\frac{1}{2}\right)\frac{\exp[-(n+1/2)\eta_0]}{\exp[(2n+1)\eta_0]-1}\right\}.$$

The induced dipole moment of an atom located at the sphere-surface point closest to the centre ($\xi' = \pi$) obtained by using the Watson transformation has the form [27]

$$\frac{\delta d_z}{d_0} = -1 + \frac{8\pi^3}{\eta_0^3}\cosh^3\left(\frac{\eta_0}{2}\right)\sum_{k=1}^{\infty}(-1)^k\frac{k^2}{\cosh(\pi^2 k/\eta_0)} + \frac{2\sqrt{2}f}{d_0}(\boldsymbol{d}_0\nabla')(A_1 - A_2)\sum_{n=0}^{\infty}\frac{n+1/2}{\exp[(2n+1)\eta_0]-1}, \quad (49)$$

where

$$(\boldsymbol{d}_0\nabla')(A_1 - A_2) = \frac{8\sqrt{2}\,d_0}{(C_{11}+2C_{12})f}\cosh^3\left(\frac{\eta_0}{2}\right) \times\sum_{n=0}^{\infty}(-1)^n\left(n+\frac{1}{2}\right)\frac{\exp[(n+1/2)\eta_0]}{\exp[(2n+1)\eta_0]-1}.$$

Due to the symmetry, the rest of the components of the dipole moment are zero in both cases: $\delta d_x = \delta d_y = 0$.

By summing series (48) and (49) with the help of the Mellin transformation, we obtain rather simple expressions for the induced dipole moment in an important particular case of two closely spaced nanospheres:

$$\frac{\delta d_z}{d_0} \approx -1 + \frac{7}{2}\zeta(3) - \frac{3\zeta^2(2)}{4[\gamma_E + \ln(2/\eta_0)]} + \frac{1}{16}\left\{7\zeta(3) + \frac{\zeta(2)}{\gamma_E + \ln(2/\eta_0)} \times\left\{1 - \frac{3}{2}\zeta(2) + \frac{\zeta(2)}{6[\gamma_E + \ln(2/\eta_0)]}\right\}\right\}\eta_0^2 + \ldots \quad (\xi' \to 0), \quad (50)$$

$$\frac{\delta d_z}{d_0} \approx -1 - \frac{2\pi^3}{\eta_0^3}(8 + 3\eta_0^2 + \ldots) \times\left[\exp\left(-\frac{\pi^2}{\eta_0}\right) - 4\exp\left(-\frac{2\pi^2}{\eta_0}\right) + \ldots\right] + \frac{2\zeta(2)}{[\gamma_E + \ln(2/\eta_0)]\eta_0^2} - \frac{1}{6[\gamma_E + \ln(2/\eta_0)]} \times\left\{1 - 5\zeta(2) + \frac{\zeta(2)}{6[\gamma_E + \ln(2/\eta_0)]}\right\} + \frac{1}{\gamma_E + \ln(2/\eta_0)} \times\left\{\frac{1}{72}[11\zeta(2) - 5] + \frac{1}{\gamma_E + \ln(2/\eta_0)}\left\{\frac{1}{432} - \frac{257}{21600}\zeta(2) + \frac{\zeta(2)}{2592[\gamma_E + \ln(2/\eta_0)]}\right\}\right\}\eta_0^2 + \ldots \quad (\xi' = \pi). \quad (51)$$

Thus, if the atom has the dipole moment directed along the line connecting two ideally conducting spheres and is located on this line on the surface of one of the spheres, the spontaneous decay rate of the atom can either infinitely increase as spheres come closer to each other (if the atom is located on the inner surface of one of the nanospheres) or take finite values (if the atom is located on the outer surface of a nanosphere). In the latter case, the spontaneous decay rate increases by a factor of $(7\zeta(3)/2)^2 \approx 17.7$ compared to the case of an atom located in a free space, which is almost twice as large as the ninefold increase in the spontaneous decay rate of the excited state of an atom located on the surface of a single sphere [15, 16].

5.4 Optical properties of an atom for large distances between spheres

In this case, expressions for the spontaneous decay rate can be obtained without the use of bispherical coordinates. The method is based on the replacement of spheres by point dipoles with polarisabilities equal to those of the corresponding spheres in a homogeneous field. This replacement is correct because in the case of large distances between spheres, the electric field near spheres is almost homogeneous. This approximation allows one to find self-consistently the dipole moments induced on spheres and reflected fields related to them. Then, by using relations (7), (8), and (10), we can obtain the expressions for the radiative and nonradiative components of the spontaneous decay rates.

We will derive the self-consistent system of equations by assuming that an atom is located at the point $\boldsymbol{r}'$ ($\boldsymbol{r}' \equiv \boldsymbol{r}_0$) and has the dipole moment $\boldsymbol{d}_0$. Let us denote the dipole moments of nanospheres by $\boldsymbol{d}_1$ and $\boldsymbol{d}_2$, respectively. For convenience, we will use the z axis as the polar axis. Let us assume that the centres of the first and second spheres are located at points with coordinates z_1 and z_2. In this case, the self-consistent system of equations for dipole moments will have the form

$$\boldsymbol{d}_1 = \alpha_1[\boldsymbol{E}_2(\boldsymbol{r}_1) + \boldsymbol{E}_0(\boldsymbol{r}_1)],$$

$$\boldsymbol{d}_2 = \alpha_2[\boldsymbol{E}_1(\boldsymbol{r}_2) + \boldsymbol{E}_0(\boldsymbol{r}_2)], \quad (52)$$

$$\boldsymbol{E}_j(\boldsymbol{r}) = -\frac{\boldsymbol{d}_j}{|\boldsymbol{r}-\boldsymbol{r}_j|^3} + 3\frac{(\boldsymbol{d}_j(\boldsymbol{r}-\boldsymbol{r}_j))(\boldsymbol{r}-\boldsymbol{r}_j)}{|\boldsymbol{r}-\boldsymbol{r}_j|^5} \quad (j = 0, 1, 2),$$

where

$$\alpha_1 = \left(\frac{\varepsilon_1 - 1}{\varepsilon_1 + 2}\right)R_1^3, \quad \alpha_2 = \left(\frac{\varepsilon_2 - 1}{\varepsilon_2 + 2}\right)R_2^3$$

are the polarisabilities of spheres.

The system can be solved in the general form, but this solution is rather cumbersome. In some characteristic cases, the expressions for induced dipole moments take a comparatively simple form. By assuming that $y' = 0$, we obtain the following expressions for different orientations of the dipole moment.

The dipole moment is oriented along the x axis ($\boldsymbol{d}_0 = d_0\boldsymbol{e}_x$):

$$d_{1x} = d_0\left[(\alpha_1\alpha_2)^{-1} - R_{12}^{-6}\right]^{-1} \times$$

$$\times\left[-\frac{1}{\alpha_2\rho_1^3}+\frac{1}{R_{12}^3\rho_2^3}+3x'^2\left(\frac{1}{\alpha_2\rho_1^5}-\frac{1}{R_{12}^3\rho_2^5}\right)\right],$$

$$d_{2x}=d_0\left[(\alpha_1\alpha_2)^{-1}-R_{12}^{-6}\right]^{-1}\times\left[-\frac{1}{\alpha_1\rho_2^3}+\frac{1}{R_{12}^3\rho_1^3}+3x'^2\left(\frac{1}{\alpha_1\rho_2^5}-\frac{1}{R_{12}^3\rho_1^5}\right)\right], \quad (53)$$

$$d_{1z}=3d_0\left[(\alpha_1\alpha_2)^{-1}-4R_{12}^{-6}\right]^{-1}\left(\frac{z'-z_1}{\alpha_2\rho_1^5}+2\frac{z'-z_2}{R_{12}^3\rho_2^5}\right)x',$$

$$d_{2z}=3d_0\left[(\alpha_1\alpha_2)^{-1}-4R_{12}^{-6}\right]^{-1}\left(\frac{z'-z_2}{\alpha_1\rho_2^5}+2\frac{z'-z_1}{R_{12}^3\rho_1^5}\right)x'. \quad (54)$$

The dipole moment is oriented along the y axis ($\boldsymbol{d}_0=d_0\boldsymbol{e}_y$):

$$d_{1y}=d_0\left[(\alpha_1\alpha_2)^{-1}-R_{12}^{-6}\right]^{-1}\left(-\frac{1}{\alpha_2\rho_1^3}+\frac{1}{R_{12}^3\rho_2^3}\right),$$

$$d_{2y}=d_0\left[(\alpha_1\alpha_2)^{-1}-R_{12}^{-6}\right]^{-1}\left(-\frac{1}{\alpha_1\rho_2^3}+\frac{1}{R_{12}^3\rho_1^3}\right). \quad (55)$$

The dipole moment is oriented along the z axis ($\boldsymbol{d}_0=d_0\boldsymbol{e}_z$):

$$d_{1x}=3d_0\left[(\alpha_1\alpha_2)^{-1}-R_{12}^{-6}\right]^{-1}\left(\frac{z'-z_1}{\alpha_2\rho_1^5}-\frac{z'-z_2}{R_{12}^3\rho_2^5}\right)x',$$

$$d_{2x}=3d_0\left[(\alpha_1\alpha_2)^{-1}-R_{12}^{-6}\right]^{-1}\left(\frac{z'-z_2}{\alpha_1\rho_2^5}-\frac{z'-z_1}{R_{12}^3\rho_1^5}\right)x', \quad (56)$$

$$d_{1z}=d_0\left[(\alpha_1\alpha_2)^{-1}-4R_{12}^{-6}\right]^{-1}\left\{-\frac{1}{\alpha_2\rho_1^3}-\frac{2}{R_{12}^3\rho_2^3}+3\left[\frac{(z'-z_1)^2}{\alpha_2\rho_1^5}+2\frac{(z'-z_2)^2}{R_{12}^3\rho_2^5}\right]\right\},$$

$$d_{2z}=d_0\left[(\alpha_1\alpha_2)^{-1}-4R_{12}^{-6}\right]^{-1}\left\{-\frac{1}{\alpha_1\rho_2^3}-\frac{2}{R_{12}^3\rho_1^3}+3\left[\frac{(z'-z_2)^2}{\alpha_1\rho_2^5}+2\frac{(z'-z_1)^2}{R_{12}^3\rho_1^5}\right]\right\}. \quad (57)$$

In (53)–(57), $\rho_{1,2}=[x'^2+(z'-z_{1,2})^2]^{1/2}$ and all other components of the induced dipole moment are zero.

A remarkable feature of expressions (53)–(57) is that they are valid for any location of the atom with respect to spheres, in particular, on their surfaces. This is explained by the fact that the dipole moment of a nanosphere in the quasi-static regime is always equal to the product of the polarisability by the dipole (atom) field at the sphere centre. The total dipole moment of the system $\boldsymbol{d}_{\text{tot}}=\boldsymbol{d}_0+\boldsymbol{d}_1+\boldsymbol{d}_2$ can be found from expressions (53)–(57), and the spontaneous decay rate – from (8).

The knowledge of the induced dipole moments of nanospheres allows us to find the excited or reflected field and then the nonradiative decay rate – from (7). In the case of $y'=0$, we have the following expressions.

The dipole moment of an atom is oriented along the x axis ($\boldsymbol{d}_0=d_0\boldsymbol{e}_x$):

$$\left(\frac{\gamma}{\gamma_0}\right)_x^{\text{nrad}}=\frac{3}{2k_0^3d_0}\,\text{Im}\left\{-\frac{d_{1x}}{\rho_1^3}-\frac{d_{2x}}{\rho_2^3}+3x'^2\left(\frac{d_{1x}}{\rho_1^5}+\frac{d_{2x}}{\rho_2^5}\right)+3x'\left[\frac{d_{1z}(z'-z_1)}{\rho_1^5}+\frac{d_{2z}(z'-z_2)}{\rho_2^5}\right]\right\}. \quad (58)$$

The dipole moment of an atom is oriented along the y axis ($\boldsymbol{d}_0=d_0\boldsymbol{e}_y$):

$$\left(\frac{\gamma}{\gamma_0}\right)_y^{\text{nrad}}=\frac{3}{2k_0^3d_0}\,\text{Im}\left(-\frac{d_{1y}}{\rho_1^3}-\frac{d_{2y}}{\rho_2^3}\right). \quad (59)$$

The dipole moment of an atom is oriented along the z axis ($\boldsymbol{d}_0=d_0\boldsymbol{e}_z$):

$$\left(\frac{\gamma}{\gamma_0}\right)_z^{\text{nrad}}=\frac{3}{2k_0^3d_0}\times\text{Im}\left\{-\frac{d_{1z}}{\rho_1^3}-\frac{d_{2z}}{\rho_2^3}+3\left[\frac{d_{1z}(z'-z_1)^2}{\rho_1^5}+\frac{d_{2z}(z'-z_2)^2}{\rho_2^5}\right]+3x'\left[\frac{d_{1x}(z'-z_1)}{\rho_1^5}+\frac{d_{2x}(z'-z_2)}{\rho_2^5}\right]\right\}. \quad (60)$$

Because expressions (58)–(60) were obtained in the dipole interaction approximation, they will coincide only with the principal terms of asymptotic expressions, which can be obtained from (17) by solving directly recurrent equations (20) and (21) within two small spheres (R_1, $R_2 \ll R_{12}$). A more accurate asymptotic expression should take into account higher-order multipole terms (quadrupole, octupole, etc.) present in the emission field of a two-nanosphere cluster, as follows from general expressions (35)–(37). In this case, the asymptotic expressions for the nonradiative component of the decay rate will be invalid when an atom is located close to one of the nanospheres. These parameters for an atom located close to a nanobody can infinitely increase [see expressions (35)–(37)], whereas they values obtained from the models of three dipoles always remain finite. The total dipole of the atom and nanosphere is calculated in the dipole interaction approximation irrespective of the atom position and the sphere material. Thus, asymptotic expressions (35)–(37) and, hence, expressions for the radiative component of the spontaneous decay rate are also valid for an atom located on the surface of one of the nanospheres.

Note also that in the case of a cluster of ideally conducting nanospheres, the asymptotic expressions for the spontaneous decay rate can be obtained from (53)–(57) by using (8) and assuming that $\varepsilon_1=\varepsilon_2\to-\infty$ ($\alpha_1=R_1^3$, $\alpha_2=R_2^3$).

5.5 Graphic illustrations and discussion of results

Figure 4 presents the wavelength dependence of the radiative component of the spontaneous decay rate of the excited state of an atom located at the centre of a cluster of two identical silver spheres. The dielectric constants of silver at different wavelengths [44] were interpolated in a standard way to provide smooth dependences. One can see that the radiative decay rate increases considerably mainly for the atom with the dipole moment directed along the z axis (Fig. 4b). When the dipole moment is directed perpendicular to the z axis, the decay rate also increases (Fig. 4a); however, unlike the atom with the longitudinal

orientation of the dipole moment, this dependence has a different type. If spheres are located close enough to each other, the transversely oriented dipole located between spheres almost does not exhibit the radiative decay. As spheres are removed from each other, the radiative component of the decay rate first increases and then slowly varies down to unity, i.e. to the value corresponding to the relative decay rate in a free space. In addition, there exist certain wavelengths at which the radiative decay rate increases considerably. This increase is caused by excitation of plasmon oscillations in the cluster, whose properties are determined by the distance between nanospheres [21]. By specifying the distance between nanoparticles, we can separate the wavelength at which the radiative component of the decay rate will increase considerably. This property can be used, for example, for the development of a new type of nanosensors based on nanoparticle pairs, which can detect individual atoms.

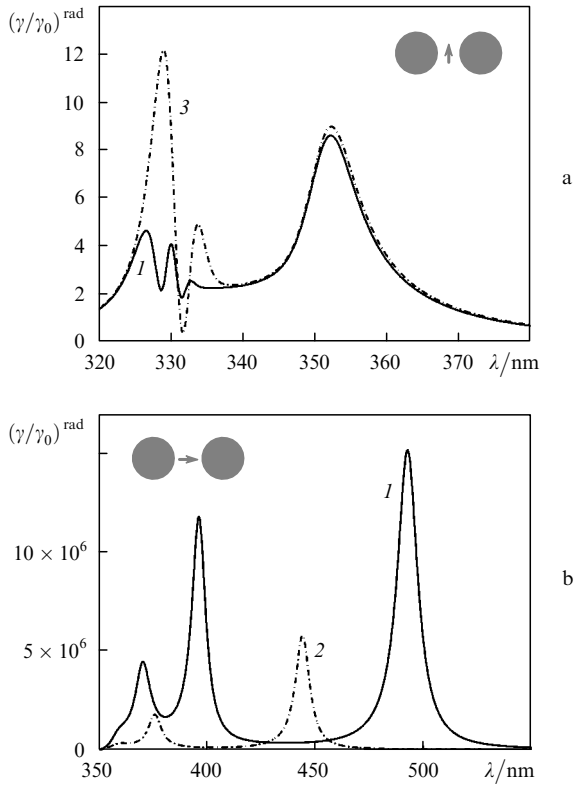

Figure 4. Wavelength dependences of the radiative component of the spontaneous decay rate for an atom located near a cluster of two silver nanospheres [44]. The atom is located at the cluster centre and has the dipole moment directed perpendicular (a) and parallel (b) to the polar axis. The radii of spheres are 50 nm and distances between their centres are $R_{12} = 101$ (*1*), 102 (*2*), and 103 nm (*3*).

Figure 5 presents the dependences of the radiative component of the spontaneous decay rate of an atom located near a cluster of two silver nanospheres ($\varepsilon = -7.06 + i0.213$ for silver at $\lambda = 450.8$ nm [44]) on the distance between the atom and cluster. One can see that, as the atom moves away from the cluster, the radiative component of the spontaneous decay rate tends to the value corresponding to the decay rate in a free space. Note that the dependences are nonmonotonic and exhibit dips in some regions of x'. The dips are observed for an atom with the transverse orientation of the dipole moment and correspond to a decrease in the radiative component of the spontaneous decay rate. For an atom with the longitudinal orientation of the dipole moment moving away from the nanosphere surface along the z axis (Fig. 5b), the dependence of the radiative component of the spontaneous decay rate is monotonic, as in the case of ideally conducting spheres.

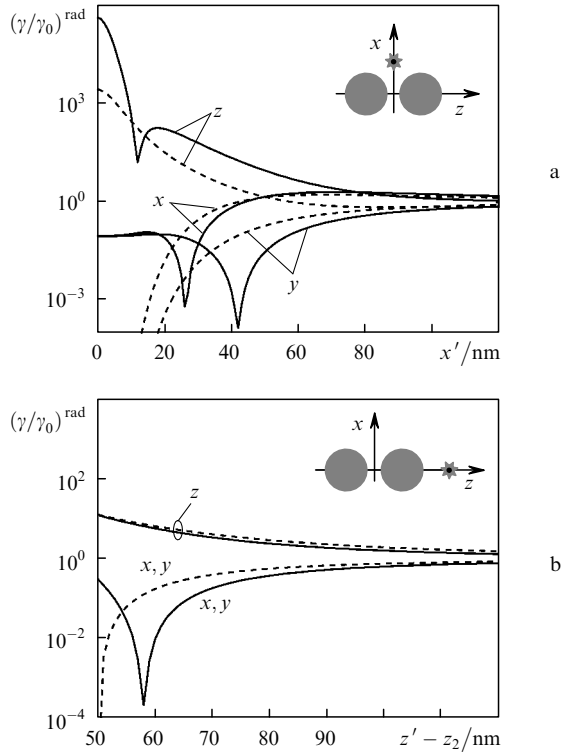

Figure 5. Dependences of the radiative component of the spontaneous decay rate on the distance from an atom to a cluster of two silver nanospheres (solid curves). The radii of spheres are 50 nm and the distance between their centres is $R_{12} = 101$ nm. The atom moves away along the x axis (a) and the z axis (b). The dipole moments of the atom are directed along axes x, y, and z. The dashed curves correspond to a cluster of two ideally conducting nanospheres.

Figure 6 shows the dependences of the nonradiative component of the decay rate on the emission wavelength. One can see that for an atom located at the centre of the cluster of silver nanospheres and having the transverse orientation of the dipole moment, the nonradiative decay will dominate, as follows from comparison with Fig. 4a. By comparing the wavelength dependences of the radiative and nonradiative components of the spontaneous decay rate of the excited state of the atom with the longitudinal orientation of the dipole moment (Figs 4b and 6b), we see that the nonradiative decay dominated at a small distance between spheres mainly in the short-wavelength (UV) spectral region. For the two resonances at wavelengths ~ 396 and ~ 493 nm for the distance between the centres of spheres equal to 101 nm, the radiative decay dominates. These two wavelengths correspond to the modes for which the charge is predominantly accumulated on the inner surface of nanospheres in the cluster [21].

Figure 7 shows the behaviour of the nonradiative component of the spontaneous decay rate of the excited state of an atom moving away from a cluster of two silver

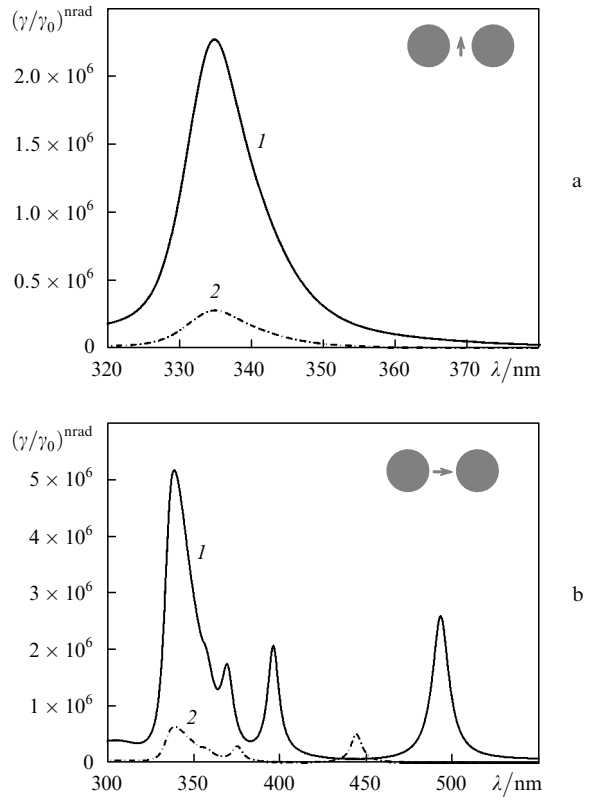

Figure 6. Wavelength dependences of the nonradiative component of the spontaneous decay rate of the exited state of an atom located near a cluster of silver nanospheres [44]. The atom is located at the cluster centre and has the dipole moment directed perpendicular (a) and parallel (b) to the polar axis. The radii of spheres are 50 nm and distances between their centres are $R_{12} = 101$ (*1*) and 102 (*2*).

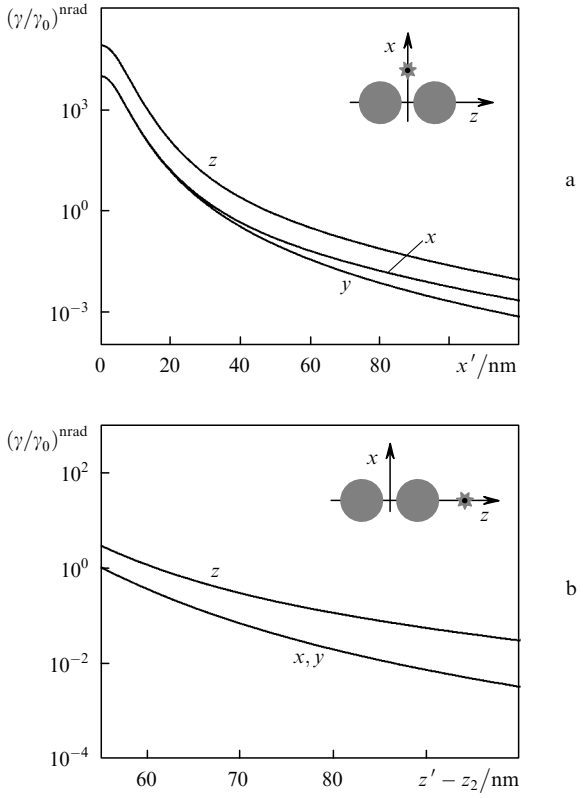

Figure 7. Dependences of the nonradiative component of the spontaneous decay rate on the distance from an atom to a cluster of two silver nanospheres. The radii of spheres are 50 nm and the distance between their centres is $R_{12} = 101$ nm. The atom moves away along the x axis (a) and z axis (b). The dipole moments of the atom are directed along the x, y, and z axes.

nanospheres with $\varepsilon = -7.06 + \text{i}0.213$ ($\lambda = 450.8$ nm [44]). One can see that the nonradiative component decreases monotonically. As the atom moves away along the z axis (polar axis) from the surface of one of the spheres (Fig. 7b), the nonradiative losses can be neglected already at a distance of $\sim 0.1R_0$ from the sphere surface because the radiative component of the spontaneous decay rate for the atom with the longitudinally oriented dipole moment in this case (cf. Fig. 5b) is almost an order of magnitude greater than the nonradiative component. For the atom with the transversely oriented dipole moment (Figs 5b and 7b), the nonradiative component of the decay rate should be taken into account because the radiative component of the decay rate considerably decreases in some region of the curve in Fig. 5b. The nonradiative component of the decay rate can be neglected already at distances $\sim 0.4R_0$ from the sphere surface. In the case of an atom with the longitudinally oriented dipole moment moving away from the cluster centre along the x axis (Fig. 7a), both the radiative and nonradiative components of the decay rate increase in the space between spheres, and the distance beginning from which the nonradiative component can be neglected is $\sim 1.6R_0$. For an atom with the transversely oriented dipole moment, this distance is approximately the same.

Although silver has a comparatively weak absorption, the structure of plasmon resonances in a cluster of two silver nanospheres is only roughly consistent with the spectra shown in Fig. 3. To demonstrate the spectra more clearly, a metal with a weaker absorption should be used. Figure 8 presents the wavelength dependences of the radiative component of the spontaneous decay rate for an atom located at the centre of a cluster of two identical nanospheres made of a hypothetical material with $\varepsilon = \varepsilon' + \text{i}\varepsilon''/30$ (where ε' and ε'' are the real and imaginary parts of the dielectric constant of silver) and located in a medium with the dielectric constant equal to unity [44]. The fine structure of resonances (Fig. 4) for a cluster of silver nanospheres is demonstrated in Fig. 8. If the dipole moment of the atom is oriented perpendicular to the polar axis, the spectrum of the radiative component of the decay rate exhibits the T and M modes (Fig. 8a), while the L modes are not excited. It is obvious that excitation of the T and M modes is explained by the symmetry of the charge induced on the surface of spheres with respect to the plane $z = 0$ [21]. If the dipole moment of the atom is directed along the polar axis (Fig. 8b), the situation changes to the opposite, and only the L modes are excited, which is in turn also explained by the symmetry of the excitation source – the charge distribution on spheres should be antisymmetric with respect to the plane $z = 0$. Note also that, as the wavelength decreases (in passing through the point corresponding to $\varepsilon' = -1$), the T modes for an atom with the transversely oriented dipole moment are changed by the M modes (Fig. 8a). In the case of excitation of an atom with the dipole moment directed along the z axis (Fig. 8b), no resonances are observed upon similar passing through the point corresponding to $\varepsilon' = -1$ and only a characteristic dip in the dependence is observed for $\varepsilon' = 0$. Note also that, if the distance between nano-

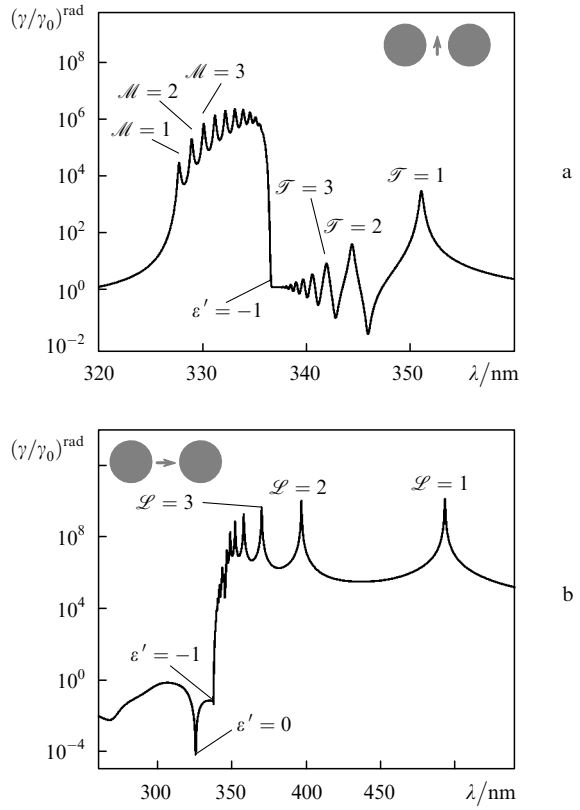

Figure 8. Wavelength dependences of the radiative component of the spontaneous decay rate for an atom located at the centre of a cluster of two nanospheres made of a hypothetical material with the dielectric constant $\varepsilon = \varepsilon' + \mathrm{i}\varepsilon''/30$, where ε' and ε'' are the real and imaginary parts of the dielectric constant of silver [44]. The dipole moment of the atom is oriented perpendicular (a) and parallel (b) to the polar axis. The radii of spheres are 50 nm and the distance between their centres is $R_{12} = 101$ nm. The resonances corresponding to excitation of the corresponding L, M, and T modes are indicated.

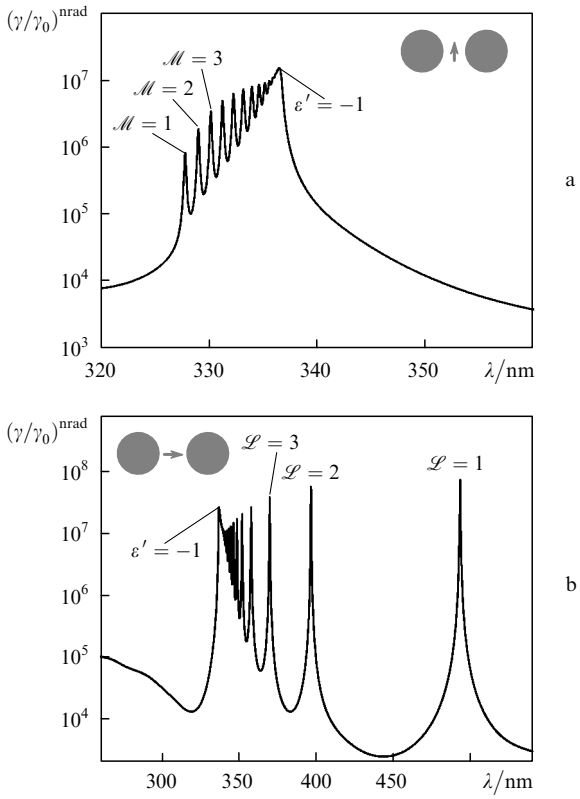

Figure 9. Wavelength dependences of the nonradiative component of the spontaneous decay rate for an atom located at the centre of a cluster of two nanospheres made of a hypothetical material of the silver type (see Fig. 8 caption). The dipole moment of the atom is oriented perpendicular (a) and parallel (b) to the polar axis. The radii of spheres are 50 nm and the distance between their centres is $R_{12} = 101$ nm.

spheres is large enough $[R_{12}/(2R_0) \geqslant 1.2]$, the radiative decay of the excited state of an atom with the transversely oriented dipole moment located at the centre of a cluster will occur only in the T modes, as follows from the corresponding dependences for the resonance dielectric constant of the M modes (Fig. 3).

Figure 9 presents the dependences of the nonradiative component of the decay rate for an atom located at the centre of a cluster of two spherical nanoparticles made of a hypothetical material of the silver type. One can see that the nonradiative decay occurs only in the M modes (Fig. 9a) and L modes (Fig. 9b). For an atom with the transversely oriented dipole moment, a slowly decaying envelope appears with increasing the wavelength (Fig. 9a) and no decay in the T modes is observed in passing through the point corresponding to $\varepsilon' = -1$. A specific feature of the T modes is that at small distances between nanospheres, the charge corresponding to the given mode is mainly concentrated on the external surface of nanospheres [21], whereas the charge is absent in fact on the internal surface (which is closest to the atom position). For this reason, the nonradiative decay in the T modes is absent (Fig. 9a).

Note that, as in the case of the radiative decay, the distribution of the surface charge with respect to the plane $z = 0$ is related to the symmetry of the source position, which results in excitation of only the M and T modes or only the L modes depending on the orientation of the dipole moment of the atom. Note also that, if the atom is displaced from the axis, one can expect that modes of all possible types will be excited both upon the radiative and nonradiative spontaneous decay of the excited state of the atom due to the change in the symmetry of the source position.

Figure 10 presents the decay rates for an atom located at the characteristic points of the system as functions of the distance between ideally conducting spheres and their asymptotics. One can see that the decay rate of an atom with the dipole moment directed along the z axis and located inside the cluster considerably increases with decreasing R_{12} (Figs 10a, b). It also follows from Fig. 10 that asymptotic expressions (47), (50) and (51) together with (53)–(60) describe the entire range of variation in the spontaneous decay rate for an atom located near two spheres.

Figure 11a presents the radiative component of the spontaneous decay rate for an atom located near a two-nanosphere cluster as a function of ε for a large distance between nanospheres. One can see that asymptotic expressions (53)–(57) for the induced dipole moment obtained in the three-dipole model (52) well describe the radiative component of the decay rate already at distances $R_{12} \simeq 4R_0$ (for identical spheres) at which nanospheres can be treated as point dipoles.

In the case of the nonradiative component of the spontaneous decay rate (Fig. 11b), asymptotic expressions (58)–(60), obtained with the help of the three-dipole model and, hence, taking into account only the dipole contribu-

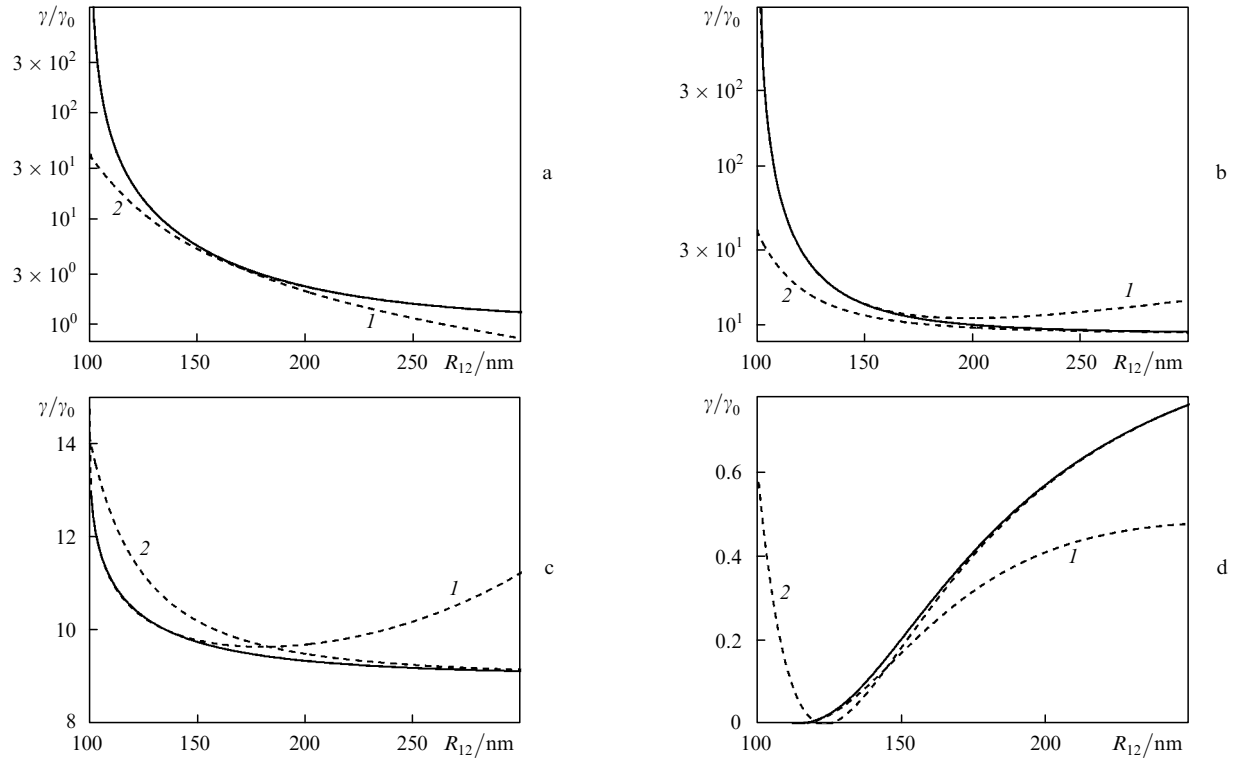

Figure 10. Dependences of the spontaneous decay rate of the excited state of an atom on the distance between two ideally conducting nanospheres (solid curves). The radii of spheres are 50 nm. The atom with the dipole moment directed along the z axis is located at the cluster centre (a), on the internal (b) or external (c) surface of one of the spheres. The atom with the dipole moment directed along the x axis is located at the cluster centre (d). Dashed curves (*1*) and (*2*) are asymptotics for $\eta \to 0$ and $\eta \to \infty$, respectively.

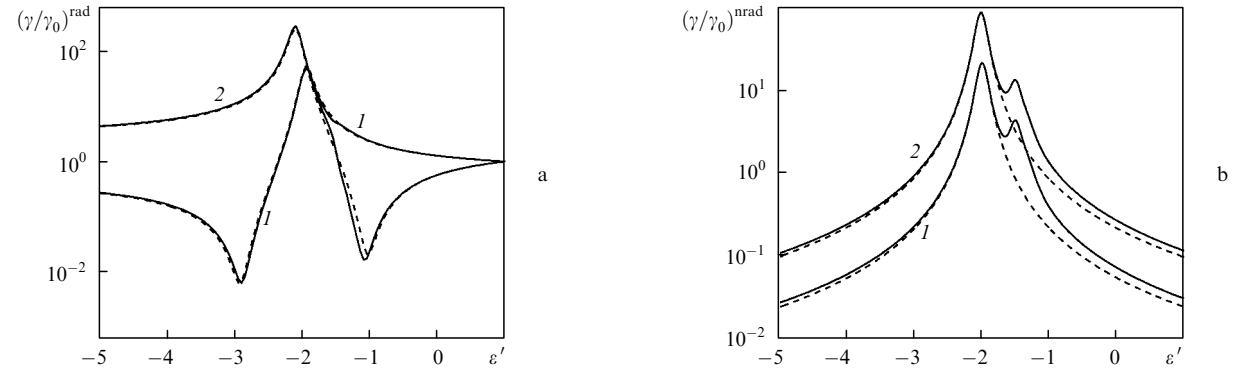

Figure 11. Asymptotic dependences obtained in the three-dipole model (52) (dashed curves) and dependences obtained by solving exactly recurrent equations (20) and (21) (solid curves) for the radiative component of the spontaneous decay rate and $R_{12} = 200$ nm (a) and the nonradiative component of the decay rate and $R_{12} = 400$ nm, $k_0 R_0 = 0.1$ (b) on the dielectric constant $\varepsilon = \varepsilon' + \mathrm{i}0.1$. The radii of spheres are 50 nm. The dipole moment of the atom is oriented perpendicular (*1*) and parallel (*2*) to the polar axis.

tion, differ from the solution obtained from recurrent equations. One can see that dipole contributions almost completely correspond to the dipole terms of the exact solution already at distances $R_{12} \geqslant 8R_0$. The resonances in the dependences corresponding to $\varepsilon' = -3/2, -4/3, \ldots$, are determined by the contributions from quadrupole, octupole, and other multipole terms. They cannot be taken into account within the framework of the three-dipole model.

So far we have considered the spontaneous decay rate by assuming that the nanoparticle radius is small compared to the emission wavelength. It is obvious that a consideration of a finite size of nanoparticles will change the form of dependences under study. Let us demonstrate this by a particular example. Figure 12 presents the radiative component of the spontaneous decay rate calculated based on the model used in our paper (solid curves) and by solving numerically the total system of Maxwell's equations (dashed curves) [26]. As an example, a cluster of two nanospheres of radii 50 nm was considered, i.e. the total size of the cluster was ~ 200 nm, which is not very small compared to the emission wavelength. It is easy to see that the consideration of a finite size of nanoparticles results in a change in the resonance amplitude and shift of the resonance wavelength. The first change is explained by the consideration of contributions from small imaginary corrections in the wave number to the resonance dielectric constant of the cluster. The shift of the resonance is determined by the contribution of real corrections.

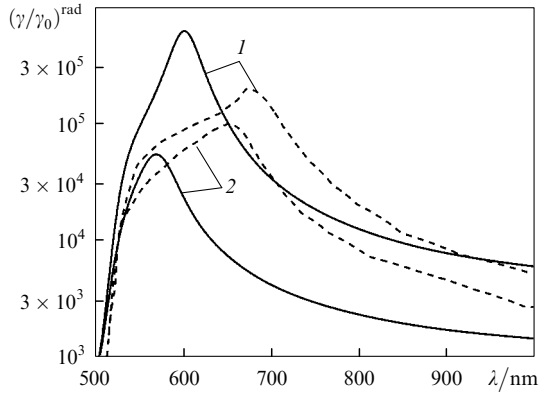

Figure 12. Wavelength dependences of the radiative component of the spontaneous decay rate for an atom located at the centre of a cluster of two gold nanospheres [44] and having the dipole moment directed along the polar axis. The dashed curves are taken from [26]. The radii of spheres are 50 nm and the distance between their centres is $R_{12} = 101$ (*1*) and 102 nm (*2*).

We demonstrated the complicated structure of plasmon resonances by using a hypothetical material of the silver type because we could not find a proper metal with small losses in the visible spectral region. However, in the IR region SiC has proper parameters due to the existence of phonon–polariton resonances [3]. Figure 13 presents the radiative component of the spontaneous decay rate for an atom located between two SiC nanospheres (the dielectric constant is taken from [45]). One can see that resonances excited in SiC and a hypothetical material (see Fig. 8) coincide qualitatively.

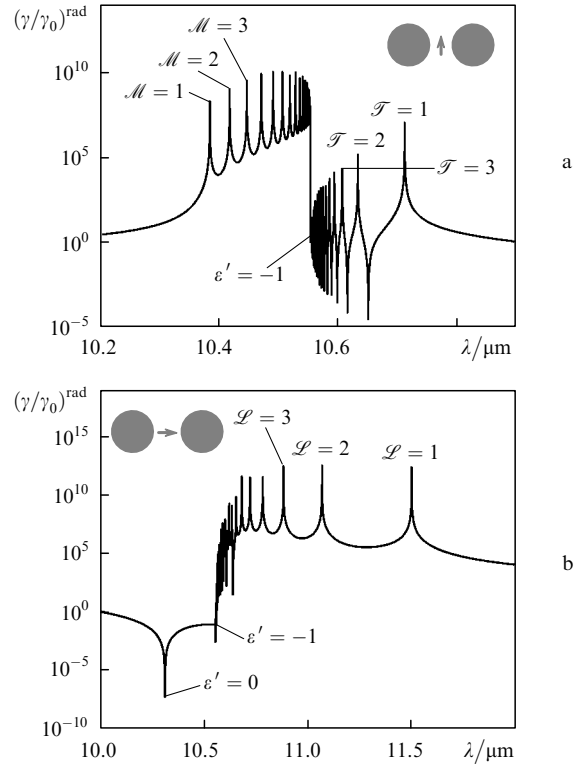

Figure 13. Wavelength dependences of the radiative component of the spontaneous decay rate for an atom located at the centre of a cluster of two SiC nanospheres [45]. The dipole moment of the atom is oriented perpendicular (a) and parallel (b) to the polar axis. The radii of spheres are 50 nm and the distance between their centres is $R_{12} = 101$ nm. The resonances corresponding to excitation of the corresponding L, M, and T modes are indicated.

6. Emission frequency shift for an atom located near a two-nanosphere cluster

6.1 Frequency shift in the general case of weakly absorbing nanospheres

In this case, the imaginary part of the Green function can be neglected compared to its real part, and according to (10), it is necessary to calculate the average dipole moment of transition between the levels under study. In the case of one-electron (hydrogen-like atoms), the expressions for averages can be obtained in the general form. Consider, for example, the transition from the P state with the wave function $|\mathrm{P}\rangle$ to the S state with the wave function $|\mathrm{S}\rangle$.

The S state is spherically symmetric, and we can easily obtain the expression

$$\langle \mathrm{S}|d_{0\alpha}d_{0\beta}|\mathrm{S}\rangle = e^2 r_0^2 \delta_{\alpha\beta}, \tag{61}$$

where $\delta_{\alpha\beta}$ is the Kronecker delta; $r_0 = \hbar^2/(m_{\rm e}e^2Z)$ is the characteristic atomic state; e and $m_{\rm e}$ are the electron charge and mass, respectively; and Z is the nucleus number in the periodic table.

The P state is triply degenerate in the projection M of the orbital quantum number, for example, on the z axis. Consider the linear combinations of the wave functions of these states in order to describe the state of an atom with a certain orientation of the dipole moment of transitions along different axes:

$$|\mathrm{P},x\rangle = \frac{|\mathrm{P},M=1\rangle + |\mathrm{P},M=-1\rangle}{\sqrt{2}},$$

$$|\mathrm{P},y\rangle = \frac{|\mathrm{P},M=1\rangle - |\mathrm{P},M=-1\rangle}{\mathrm{i}\sqrt{2}}, \tag{62}$$

$$|\mathrm{P},z\rangle = |\mathrm{P},M=0\rangle.$$

For these states,

$$\langle \mathrm{P},x|d_{0\alpha}d_{0\beta}|\mathrm{P},x\rangle = 6e^2r_0^2\begin{bmatrix}3&0&0\\0&1&0\\0&0&1\end{bmatrix}, \tag{63}$$

$$\langle \mathrm{P},y|d_{0\alpha}d_{0\beta}|\mathrm{P},y\rangle = 6e^2r_0^2\begin{bmatrix}1&0&0\\0&3&0\\0&0&1\end{bmatrix}, \tag{64}$$

$$\langle \mathrm{P},z|d_{0\alpha}d_{0\beta}|\mathrm{P},z\rangle = 6e^2r_0^2\begin{bmatrix}1&0&0\\0&1&0\\0&0&3\end{bmatrix}. \tag{65}$$

Thus, only diagonal terms of the Green function $G^{(0)}_{\alpha\beta}(\boldsymbol{r}', \boldsymbol{r}')$ ($\alpha = \beta$) will contribute to the $\mathrm{P} \to \mathrm{S}$ transition. Therefore, according to (10), the emission frequency shift for different orientations of the dipole moment will be described by the expressions

$$\Delta\omega_x = -\frac{1}{2\hbar}\, e^2 r_0^2 \mathrm{Re}\left[17G^{(0)}_{xx} + 5G^{(0)}_{yy} + 5G^{(0)}_{zz}\right],$$

$$\Delta\omega_y = -\frac{1}{2\hbar}\, e^2 r_0^2 \mathrm{Re}\big[5G_{xx}^{(0)} + 17G_{yy}^{(0)} + 5G_{zz}^{(0)}\big], \qquad (66)$$

$$\Delta\omega_z = -\frac{1}{2\hbar}\, e^2 r_0^2 \mathrm{Re}\big[5G_{xx}^{(0)} + 5G_{yy}^{(0)} + 17G_{zz}^{(0)}\big].$$

In the case of a classical (Lorentzian) atom, the emission frequency shift with respect to the central axis ω_0 is described by the expression [38]

$$\frac{\omega-\omega_0}{\gamma_0} = -\frac{3}{4k_0^3 d_0^2}\,\mathrm{Re}[d_{0\alpha}d_{0\beta}G_{\alpha\beta}^{(0)}(\boldsymbol{r}',\boldsymbol{r}') + \ldots]. \qquad (67)$$

For particular cases of the orientation of the transition dipole moment, we have the expressions

$$\Delta\omega_x = -\frac{3\gamma_0}{4k_0^3}\,\mathrm{Re}\,G_{xx}^{(0)},$$

$$\Delta\omega_y = -\frac{3\gamma_0}{4k_0^3}\,\mathrm{Re}\,G_{yy}^{(0)}, \qquad (68)$$

$$\Delta\omega_z = -\frac{3\gamma_0}{4k_0^3}\,\mathrm{Re}\,G_{zz}^{(0)}.$$

By comparing (66) and (68), we can easily see that, knowing classical frequency shifts (68), it is easy to find their quantum-mechanical analogues (66). Therefore, without loss of generality, we will consider below classical expression (67) for the frequency shift.

By comparing expression (7) for the nonradiative component of the decay rate with expression (67) for the frequency shift, we see that to find the principal term in (67), which is determined by the quasi-static contribution of the field in expressions (35)–(37), it is necessary to replace factors $\mathrm{Im}\{\ldots\}$ by factors $\mathrm{Re}\{\ldots\}$ and multiply the obtained expressions by $-1/2$. Therefore, we will not present these expressions here.

6.2 Frequency shift of spontaneous emission in the case of ideally conducting nanospheres

In the case of ideally conducting nanospheres, we can obtain from (67) the explicit expressions of the frequency shift. For this purpose, it is necessary to determine the reflected field at the atom location point. In the general case of nanospheres of different radii, these expressions prove to be extremely cumbersome; therefore, it is reasonable to consider a particular case of two identical nanospheres. In this particular case, we obtain the following expressions ($\varphi' = 0$) [28].

The dipole moment of an atom is oriented along the x axis ($\boldsymbol{d}_0 = d_0\boldsymbol{e}_x$):

(a) the atom is located on the x axis ($\eta' = 0$):

$$\frac{\omega-\omega_0}{\gamma_0} = -\frac{3}{4k_0^3}\,\mathrm{Re}\,G_{xx}^{(0)}(x',x') = -\frac{3(1-\cos\xi')}{4(k_0 f)^3}$$

$$\times\Bigg\{\frac{1}{2}\sin^2\xi'\sum_{n=0}^{\infty}\sum_{m=0}^{n}[2-\delta(m,0)]\frac{(n-m)!}{(n+m)!}\frac{[P_n^m(\cos\xi')]^2}{\exp[(2n+1)\eta_0]+1}$$

$$+(1-\cos\xi')\sin\xi'\sum_{n=0}^{\infty}\sum_{m=0}^{n}[2-\delta(m,0)]\frac{(n-m)!}{(n+m)!}\times$$

$$\times\frac{1}{\exp[(2n+1)\eta_0]+1}\frac{\partial[P_n^m(\cos\xi')]^2}{\partial\xi'} + 2(1-\cos\xi')^2$$

$$\times\sum_{n=0}^{\infty}\sum_{m=0}^{n}[2-\delta(m,0)]\frac{(n-m)!}{(n+m)!}\frac{1}{\exp[(2n+1)\eta_0]+1}$$

$$\times\left[\frac{\partial P_n^m(\cos\xi')}{\partial\xi'}\right]^2\Bigg\} + \frac{3(1-\cos\xi')}{C_{11}(k_0 f)^3}$$

$$\times\Bigg\{\frac{1}{2}\sin\xi'\sum_{n=0}^{\infty}\frac{P_n(\cos\xi')}{\exp[(2n+1)\eta_0]+1} + (1-\cos\xi')$$

$$\times\sum_{n=0}^{\infty}\frac{1}{\exp[(2n+1)\eta_0]+1}\frac{\partial P_n(\cos\xi')}{\partial\xi'}\Bigg\}^2; \qquad (69)$$

(b) the atom is located on the z axis:

$$\frac{\omega-\omega_0}{\gamma_0} = -\frac{3}{4k_0^3}\,\mathrm{Re}\,G_{xx}^{(0)}(z',z') = -\frac{3(\cosh\eta'\pm 1)^3}{4(k_0 f)^3} \qquad (70)$$

$$\times\sum_{n=1}^{\infty}n(n+1)\left\{\frac{\cosh^2[(n+1/2)\eta']}{\exp[(2n+1)\eta_0]+1} + \frac{\sinh^2[(n+1/2)\eta']}{\exp[(2n+1)\eta_0]-1}\right\},$$

where the upper sign corresponds to the atom located between spheres ($\xi' = \pi$) and the lower sign – to the atom located behind one of the spheres ($\xi' \to 0$).

The dipole moment of an atom is oriented along the y axis ($\boldsymbol{d}_0 = d_0\boldsymbol{e}_y$):

the atom is located on the x axis ($\eta' = 0$):

$$\frac{\omega-\omega_0}{\gamma_0} = -\frac{3}{4k_0^3}\,\mathrm{Re}\,G_{yy}^{(0)}(x',x') = -\frac{3(1-\cos\xi')^3}{(k_0 f)^3\sin^2\xi'}$$

$$\times\sum_{n=1}^{\infty}\sum_{m=1}^{n}m^2\frac{(n-m)!}{(n+m)!}\frac{[P_n^m(\cos\xi')]^2}{\exp[(2n+1)\eta_0]+1}. \qquad (71)$$

The cases when the atom is located on the z axis between spheres and behind one of the spheres are identical to cases described by expression (70).

The dipole moment of an atom is oriented along the z axis ($\boldsymbol{d}_0 = d_0\boldsymbol{e}_z$):

(a) the atom is located on the x axis ($\eta' = 0$):

$$\frac{\omega-\omega_0}{\gamma_0} = -\frac{3}{4k_0^3}\,\mathrm{Re}\,G_{zz}^{(0)}(x',x') = -\frac{3(1-\cos\xi')^3}{2(k_0 f)^3} \qquad (72)$$

$$\times\sum_{n=0}^{\infty}\sum_{m=0}^{n}[2-\delta(m,0)]\frac{(n-m)!}{(n+m)!}\left(n+\frac{1}{2}\right)^2\frac{[P_n^m(\cos\xi')]^2}{\exp[(2n+1)\eta_0]-1}$$

$$+\frac{3(1-\cos\xi')^3}{(k_0 f)^3(2C_{12}+C_{11})}\left\{\sum_{n=0}^{\infty}\left(n+\frac{1}{2}\right)\frac{P_n(\cos\xi')}{\exp[(2n+1)\eta_0]-1}\right\}^2;$$

(b) the atom is located on the z axis:

$$\frac{\omega-\omega_0}{\gamma_0} = -\frac{3}{4k_0^3}\,\mathrm{Re}\,G_{zz}^{(0)}(z',z') = -\frac{3(\cosh\eta'\pm 1)}{2(k_0 f)^3}$$

$$\times\big(\tilde{A}_1\tilde{B}_1 + \tilde{A}_2\tilde{B}_2\big) - \frac{3(\cosh\eta'\pm 1)}{4(k_0 f)^3}$$

$$\times\Bigg\{\frac{1}{2}\sinh^2\eta'\sum_{n=0}^{\infty}\left\{\frac{\cosh^2[(n+1/2)\eta']}{\exp[(2n+1)\eta_0]+1} +\right.$$

$$+\frac{\sinh^2[(n+1/2)\eta']}{\exp[(2n+1)\eta_0]-1}\Bigg\}+\sinh\eta'(\cosh\eta'\pm1)\sum_{n=0}^{\infty}\left(n+\frac{1}{2}\right)$$

$$\times\sinh[(2n+1)\eta']\Bigg\{\frac{1}{\exp[(2n+1)\eta_0]+1}$$

$$+\frac{1}{\exp[(2n+1)\eta_0]-1}\Bigg\}+2(\cosh\eta'\pm1)^2\sum_{n=0}^{\infty}\left(n+\frac{1}{2}\right)^2$$

$$\times\Bigg\{\frac{\sinh^2[(n+1/2)\eta']}{\exp[(2n+1)\eta_0]+1}+\frac{\cosh^2[(n+1/2)\eta']}{\exp[(2n+1)\eta_0]-1}\Bigg\}\Bigg\}, \quad (73)$$

where

$$\tilde{A}_1=-\frac{C_{11}\tilde{B}_1+C_{12}(\tilde{B}_1+\tilde{B}_2)}{(2C_{12}+C_{11})C_{11}};$$

$$\tilde{A}_2=-\frac{C_{12}(\tilde{B}_1+\tilde{B}_2)+C_{11}\tilde{B}_2}{(2C_{12}+C_{11})C_{11}}; \quad (74)$$

the expressions for C_{11} and C_{12} are presented in (43);

$$\tilde{B}_1=\frac{1}{2}\sinh\eta'\sum_{n=0}^{\infty}(-1)^n\Bigg\{\frac{\cosh[(n+1/2)\eta']}{\exp[(2n+1)\eta_0]+1}$$

$$-\frac{\sinh[(n+1/2)\eta']}{\exp[(2n+1)\eta_0]-1}\Bigg\}+(\cosh\eta'\pm1)\sum_{n=0}^{\infty}(-1)^n\left(n+\frac{1}{2}\right)$$

$$\times\Bigg\{\frac{\sinh[(n+1/2)\eta']}{\exp[(2n+1)\eta_0]+1}-\frac{\cosh[(n+1/2)\eta']}{\exp[(2n+1)\eta_0]-1}\Bigg\}; \quad (75)$$

$$\tilde{B}_2=\frac{1}{2}\sinh\eta'\sum_{n=0}^{\infty}(-1)^n\Bigg\{\frac{\cosh[(n+1/2)\eta']}{\exp[(2n+1)\eta_0]+1}$$

$$+\frac{\sinh[(n+1/2)\eta']}{\exp[(2n+1)\eta_0]-1}\Bigg\}+(\cosh\eta'\pm1)\sum_{n=0}^{\infty}(-1)^n\left(n+\frac{1}{2}\right)$$

$$\times\Bigg\{\frac{\sinh[(n+1/2)\eta']}{\exp[(2n+1)\eta_0]+1}+\frac{\cosh[(n+1/2)\eta']}{\exp[(2n+1)\eta_0]-1}\Bigg\}. \quad (76)$$

The upper sign in expressions (73), (75), and (76) corresponds to the atom located between spheres ($\xi'=\pi$) and the lower sign – to the atom located behind one of the spheres ($\xi'\to0$).

6.2.1 Asymptotic expressions at small distances between spheres

In the case of small distances between spheres, it is possible to obtain simple asymptotic expressions for the frequency shift not using general expressions (69)–(73). Nevertheless, the summation of series appearing in calculations is not always possible. Consider a particular case, when an atom is located midway between spheres coming closer together. By using, for example, expressions (71) and (72), we obtain the following relations ($\varphi'=0$).

The dipole moment of an atom is oriented perpendicular to the polar axis:

$$\frac{\omega-\omega_0}{\gamma_0}=-\frac{6}{(k_0f)^3}\sum_{n=0}^{\infty}\frac{n(n+1)}{\exp[(2n+1)\eta_0]+1}. \quad (77)$$

The dipole moment of an atom is oriented parallel to the polar axis:

$$\frac{\omega-\omega_0}{\gamma_0}=-\frac{12}{(k_0f)^3}\sum_{n=0}^{\infty}\frac{(n+1/2)^2}{\exp[(2n+1)\eta_0]-1}$$

$$+\frac{24}{(2C_{12}+C_{11})(k_0f)^3}\left\{\sum_{n=0}^{\infty}(-1)^n\frac{n+1/2}{\exp[(2n+1)\eta_0]-1}\right\}^2. \quad (78)$$

In the case of two spheres approaching each other ($\eta_0\to0$), expressions (77) and (78) can be summed by using the Mellin transformation. As a result, we obtain the following expressions [28].

The dipole moment of an atom is oriented perpendicular to the polar axis:

$$\frac{\omega-\omega_0}{\gamma_0}=-\frac{1}{(k_0R_0)^3}\Bigg\{\frac{9\zeta(3)}{8\eta_0^6}-\frac{3}{16\eta_0^4}[3\zeta(3)+4\ln2]$$

$$+\frac{1}{320\eta_0^2}[51\zeta(3)+120\ln2+17]$$

$$-\frac{1}{160}\left[\frac{457}{84}\zeta(3)+17\ln2+\frac{1685}{504}\right]+\ldots\Bigg\}. \quad (79)$$

The dipole moment of an atom is oriented parallel to the polar axis:

$$\frac{\omega-\omega_0}{\gamma_0}=-\frac{1}{(k_0R_0)^3}$$

$$\times\Bigg\{\frac{3\zeta(3)}{\eta_0^6}-\frac{1}{2\eta_0^4}\left[3\zeta(3)+\frac{3}{\gamma_E+\ln(2/\eta_0)}-1\right]+\frac{1}{480\eta_0^2}$$

$$\times\Bigg\{204\zeta(3)+\frac{10}{\gamma_E+\ln(2/\eta_0)}\left[30+\frac{1}{\gamma_E+\ln(2/\eta_0)}\right]-127\Bigg\}$$

$$-\frac{1}{604800}\Bigg\{54840\zeta(3)+\frac{1}{\gamma_E+\ln(2/\eta_0)}\Bigg\{103320 \quad (80)$$

$$+\frac{1}{\gamma_E+\ln(2/\eta_0)}\left[5103+\frac{175}{\gamma_E+\ln(2/\eta_0)}\right]\Bigg\}-46940\Bigg\}+\ldots\Bigg\}.$$

One can see from expressions (79) and (80) that the frequency shift of spontaneous emission of an atom located between two nanospheres approaching each other increases infinitely according to a power law. In this case, if the distance between spheres is small enough, the frequency shift for an atom with the dipole moment directed along the polar axis occurs $8/3\approx2.7$ times faster than for an atom with the dipole moment directed perpendicular to this axis. This can be explained by the fact that the normal component of the reflected field near a nanosphere at the dipole location point is greater than the tangential component.

Note that the principal terms of asymptotic expressions (78) and (79) correspond to the solution of the problem about the emission frequency shift for an atom located between two ideally conducting parallel planes. Indeed, by multiplying expressions (39) and (40) by $-1/2$ and replacing in them the factors $\mathrm{Im}\{\ldots\}$ by factors $\mathrm{Re}\{\ldots\}$, we obtain the principal terms of expressions (79) and (80), respectively,

in a particular case of and atom located midway ($z' = 0$) between two ideally conducting planes ($\beta_1 = \beta_2 = 1$).

6.2.2 Asymptotic expressions at large distances between spheres

Asymptotic expressions for the frequency shift at large distances between spheres can be obtained from expressions (58)–(60) by replacing in them the factors Im{...} by factors Re{...} and multiplying the obtained expressions by $-1/2$. Therefore, we will not present these expressions here.

6.3 Graphic illustrations and discussion

Figure 14 presents the wavelength dependences of the spontaneous-emission frequency shift of an atom located near a cluster of two identical silver nanospheres [44]. One can see that the frequency shift can be both positive and negative, and at some wavelengths for the distance between the centres of nanospheres equal to 101 nm it can be zero. The latter circumstance can be important in the design of nanosensors based on clusters of spherical silver nanoparticles.

Figure 15 shows the emission frequency shift for an atom as a function of the distance from the atom to a cluster of two silver nanospheres. Also, the dependences for ideally conducting spheres are presented (dashed curves). One can see that frequency shifts for the atom moving away along the x axis (Fig. 15a) in the cases of silver or ideally conducting nanospheres almost coincide. This is explained by the fact that the real part of the dielectric constant of silver at a wavelength of 450.8 nm is rather large compared to the imaginary part. This relation changes for other wavelengths, resulting in the change in the frequency shift, which can be negative, positive or close to zero. Note also that, as for a cluster of ideally conducting spheres, in the case of a cluster of metal spheres, the frequency shift for the atom with the longitudinally oriented dipole moment occurs faster than for the atom with the transversely oriented dipole moment.

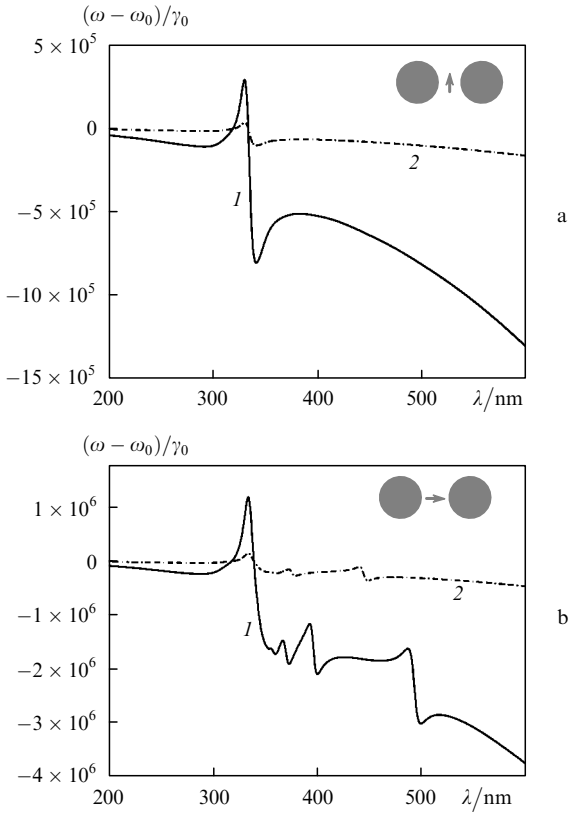

Figure 14. Wavelength dependences of the spontaneous-emission frequency shift for an atom located near a cluster of two silver nanospheres [44]. The atom is located at the cluster centre and has the dipole moment directed perpendicular (a) and parallel (b) to the polar axis. The radii of spheres are 50 nm and distances between their centres are $R_{12} = 101$ (*1*) and 102 nm (*2*).

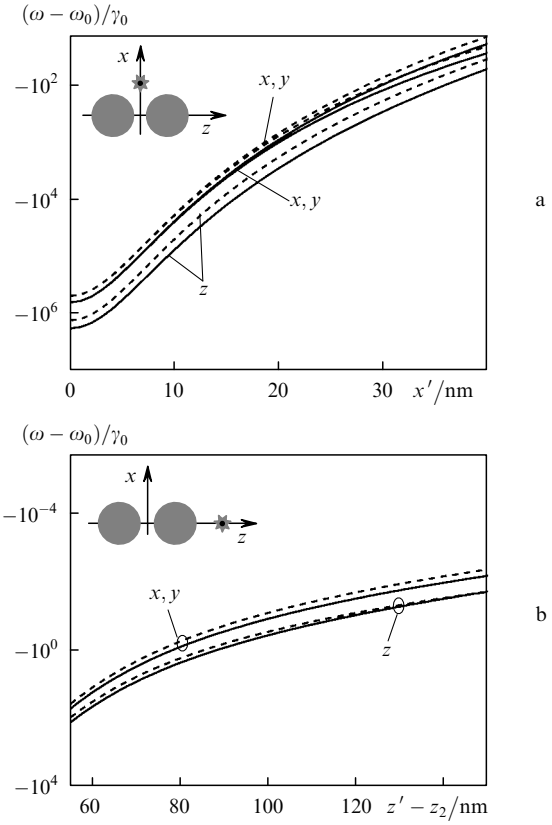

Figure 15. Dependences of the spontaneous-emission frequency shift of an atom on the distance between the atom and a cluster of two silver nanospheres (solid curves). The radii of spheres are 50 nm and the distance between their centres is $R_{12} = 101$ nm. The atom moves away along the x (a) and z (b) axes. The dipole moment of the atom is directed along axes x, y, and z. The dashed curves show the frequency shift for the atom located near ideally conducting spheres.

Figure 16 presents the wavelength dependences of the spontaneous-emission frequency shift for the atom located at the centre of a cluster of two spherical nanoparticles made of a hypothetical material with the dielectric constant $\varepsilon = \varepsilon' + i\varepsilon''/30$ (ε' and ε'' are the real and imaginary parts of the dielectric constant of silver [44]). One can see that, as for the nonradiative component of the spontaneous decay rate (Fig. 9), only resonances corresponding to the M (Fig. 16a) and L modes (Fig. 16b) are excited and no decay at the T modes is observed.

Figure 17 shows the dependences of the emission frequency shift for an atom located at the centre of a cluster with the dipole moment directed perpendicular (Fig. 17a) and parallel (Fig. 17b) to the polar axis on the distance between ideally conducting spheres. Also, the corresponding asymptotics are presented for small [(79) and (80)] and large

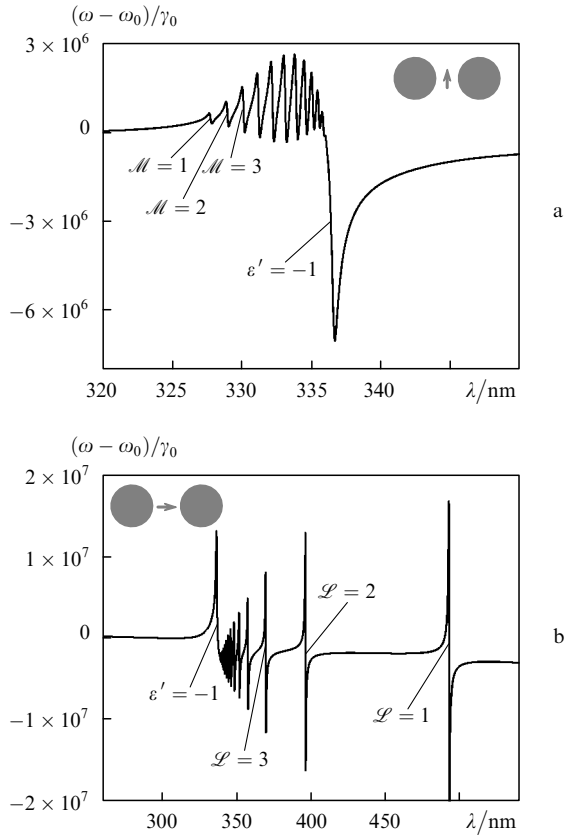

Figure 16. Wavelength dependences of the spontaneous-emission frequency shift of an atom located at the centre of a cluster of two nanospheres made of a hypothetical material of the silver type (see Fig. 8 caption). The dipole moment of the atom is oriented perpendicular (a) and parallel (b) to the polar axis. The radii of spheres are 50 nm and the distance between their centres is $R_{12}=101$ nm. The resonance wavelength corresponding to excitation of the L and M modes are indicated.

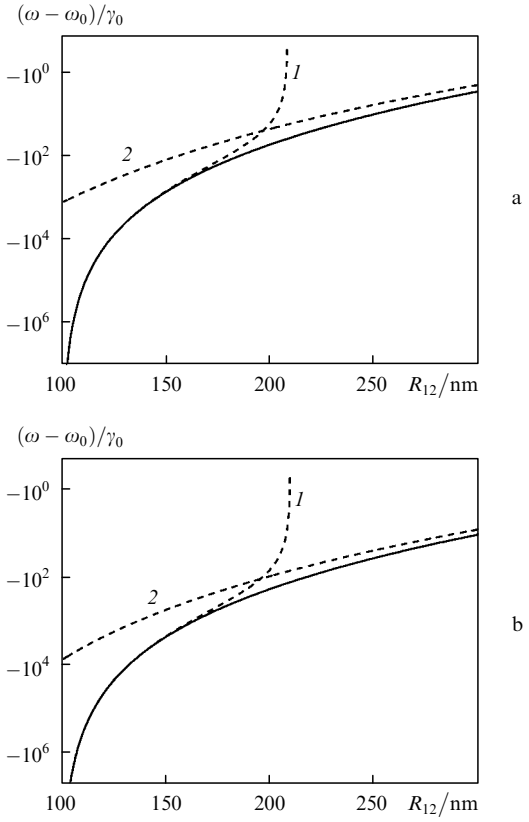

Figure 17. Dependences of the spontaneous-emission frequency shift for an atom (molecule) on the distance between ideally conducting nanospheres of the cluster (solid curves). The radii of spheres are 50 nm and $k_0R_0=0.1$. The dipole moment of the atom located at the cluster centre is directed along the z (a) and x (b) axes. The dashed curves (*1*) and (*2*) are asymptotics for $\eta_0\to0$ and $\eta_0\to\infty$, respectively.

[(58)–(60)] distances between spheres. One can see that, as for the spontaneous decay rate, the use of asymptotic expressions allows one to describe the entire range of the emission frequency shift of the atom.

7. Conclusions

We have studied in the quasi-static approximation the spontaneous decay rates of the excited state of an atom (molecule) located near a cluster of two arbitrarily arranged nanospheres of an arbitrary composition. The theory developed in the paper gives the decay rates for different orientations of the dipole moment and different arrangements of the atomic dipole with respect to the cluster. It is shown that the decay rate considerably increases at the resonance frequencies corresponding to the plasmon frequencies of the cluster, which are determined by the mutual arrangement of nanospheres. The maximum increase in the spontaneous decay rate takes place for an atom located at the cluster centre at small distances between nanospheres. It has been found that, by varying the distance between nanospheres in the cluster, it is possible to control efficiently the spontaneous decay rate for the atom located between spheres. This can be used for the development of a new type of nanosensors based on nanoparticles pairs, which can be applied for detecting individual atoms (molecules) with a high signal-to-noise ratio because nanosensors of this type will be low-sensitive to homogeneous external fields. We have investigated the emission frequency shift for an atom located at an arbitrary point and having in the general case the dipole moment arbitrarily oriented with respect to the cluster. The asymptotic expressions for the spontaneous decay rate and frequency shift have been considered. It has been shown that already for distances between the centres of identical nanospheres exceeding eight nanosphere radii, the principal contributions to the parameters under study can be calculated by using the model in which spheres are replaced by point dipoles with polarisabilities equal to the polarisability of each of the spheres in a homogeneous field.

As a whole, the results obtained in the paper allow us to estimate promptly the optical properties of a two-nanosphere cluster and their influence on the optical properties of atoms and molecules.

Acknowledgements. This work was partially supported by the Russian Foundation for Basic Research (Grant Nos 07-02-01328 and 05-02-19647) and the program of the Presidium of RAS 'Quantum Macrophysics'. One of the authors (D.V.G.) also acknowledges the partial support of the scientific training program of Lebedev Physics Institute and the program of the Presidium of RAS for the Support of Young Scientists.

References

1. Raether H. *Surface Plasmons* (Berlin: Springer-Verlag, 1998).
2. Kreibig U., Vollmer M. *Optical Properties of Metal Clusters* (Berlin: Springer-Verlag, 1995).
3. Hillenbrand R., Taubner T., Keilmann F. *Nature*, **418**, 159 (2002).
4. Moskovits M., Tay L.-L., Yang J., Haslett T. *Top. Appl. Phys.*, **82**, 215 (2002).
5. Liu Y., Bishop J., Williams L., Blair S., Herron J. *Nanotechnology*, **15**, 1368 (2004).
6. Chah S., Hammond M.R., Zare R.N. *Chemistry & Biology*, **12**, 323 (2005).
7. Brongersma M. *Nat. Mater.*, **2**, 296 (2003).
8. Protsenko I.E., Uskov A.V., Zaimidoroga O.A., Samoilov V.N., O'Reilly E.P. *Phys. Rev. A*, **71**, 063812 (2005).
9. Klimov V.V., Ducloy M., Letokhov V.S. *Chem. Phys. Lett.*, **358**, 192 (2002).
10. Lakowicz J.R., Malicka J., Gryczynski I., Gryczynski Z., Geddes C.D. *J. Phys. D: Appl. Phys.*, **36**, R240 (2003).
11. Kneipp K., Kneipp H., Itzkan I., Dasari R.R., Feld M.S. *Chem. Rev.*, **99**, 2957 (1999).
12. Xu H.X., Bjerneld E.J., Kall M., Borjesson L. *Phys. Rev. Lett.*, **83**, 4357 (1999).
13. Vo-Dinh T. *Trends Anal. Chem.*, **17**, 557 (1998).
14. *Nanophotonics: Assessment of Technology and Market Opportunities* (Mountain View, CA: Strategies Unlimited, 2005).
15. Klimov V.V., Ducloy M., Letokhov V.S. *Kvantovaya Elektron.*, **31**, 569 (2001) [*Quantum Electron,* **31**, 569 (2001)].
16. Klimov V.V. *Usp. Fiz. Nauk*, **173**, 1008 (2003).
17. Klimov V.V., Ducloy M. *Phys. Rev. A*, **69**, 013812 (2004).
18. Metiu H. *Prog. Surf. Sci.*, **17**, 153 (1984).
19. Guzatov D.V., Klimov V.V. *Chem. Phys. Lett.*, **412**, 341 (2005).
20. Nordlander P., Oubre C., Prodan E., Li K., Stockman M.I. *Nano Lett.*, **4**, 899 (2004).
21. Klimov V.V., Guzatov D.V. *Phys. Rev. B*, **75**, 024303 (2007).
22. Olivares I., Rojas R., Claro F. *Phys. Rev. B*, **35**, 2453 (1987).
23. Claro F. *Phys. Rev. B*, **25**, 7875 (1982).
24. Ruppin R. *Phys. Rev. B*, **26**, 3440 (1982).
25. Ruppin R. *J. Phys. Soc. Jpn1*, **58**, 1446 (1989).
26. Blanco L.A., Garcia de Abajo F.J. *J. Quant. Spectr. Rad. Transfer*, **89**, 37 (2004).
27. Guzatov D.V., Klimov V.V. *Kvantovaya Elektron.*, **35**, 891 (2005) [*Quantum Electron*, **35**, 891 (2005)].
28. Guzatov D.V. *Kvantovaya Elektron.*, **35**, 901 (2005) [*Quantum Electron*, **35**, 901 (2005)].
29. Paley A.V., Radchik A.V., Smith G.B. *J. Appl. Phys.*, **73**, 3446 (1993).
30. Xu H., Kall M. *Phys. Rev. Lett.*, **89**, 246802 (2002).
31. Genov D.A., Sarychev A.K., Shalaev V.M., Wei A. *Nano Lett.*, **4**, 153 (2004).
32. Chaumet P.C., Dufour J.P. *J. Electrostat.*, **43**, 145 (1998).
33. Su K.-H., Wei Q.-H., Zhang X. *Nano Lett.*, **3**, 1087 (2003).
34. Rechberger W., Hohenau A., Leitner A., Krenn J.R., Lamprecht B., Aussenegg F.R. *Opt. Commun.*, **220**, 137 (2003).
35. Tamaru H., Kuwata H., Miyazaki H.T., Miyano K. *Appl. Phys. Lett.*, **80**, 1826 (2002).
36. Prikulis J., Svedberg F., Kall M., Enger J., Ramser K., Goksor M., Hanstorp D. *Nano Lett.*, **4**, 115 (2004).
37. Wylie J.M., Sipe J.E. *Phys. Rev. A*, **30**, 1185 (1984).
38. Haroshe S., in *Fundamental Systems in Quantum Optics* (Amsterdam: Elsevier, 1992).
39. Chance R.R., Prock A., Sylbey R. *Adv. Chem. Phys.*, **37**, 1 (1978).
40. Wylie J.M., Sipe J.E. *Phys. Rev. A*, **32**, 2030 (1985).
41. Stevenson A.F. *J. Appl. Phys.*, **24**, 1134 (1953).
42. Buchholtz H. *Elektrische und Magnetische Potentialfelder* (Berlin: Springer-Verlag, 1957; Moscow: Inostrannaya Literatura, 1961).
43. Morse P.M., Feshbach H. *Methods of Theoretical Physics* (New York: McGraw-Hill, 1953; Moscow: Inostrannaya Literatura, 1960).
44. Johnson P.B., Christy R.W. *Phys. Rev. B*, **6**, 4370 (1972).
45. Engelbrecht F., Helbig R. *Phys. Rev. B*, **48**, 698 (1993).